

**STUDY OF THE MICRO UNMANNED AERIAL VEHICLE (MUAV) VERTICAL  
TAKE-OFF AND LANDING (VTOL) CONTROL SYSTEM**

By

Mohd Syafiqrul Ikhwan Bin Mohd Zulkifli

Dissertation submitted in partial fulfillment of  
the requirement for the  
Bachelor of Engineering (Hons)  
(Mechanical Engineering)

MAY 2011

Universiti Teknologi PETRONAS

Bandar Seri Iskandar

31750 Tronoh

Perak Darul Ridzuan

CERTIFICATION OF APPROVAL


Study of the Micro Unmanned Aerial Vehicle (MUAV) Vertical Take-off and Landing  
(VTOL) Control System

by

Mohd Syafiqrul Ikhwan bin Mohd Zulkifli

A project dissertation submitted to the  
Mechanical Engineering Programme  
Universiti Teknologi PETRONAS  
in partial fulfilment of the requirement for the  
BACHELOR OF ENGINEERING (Hons)  
(MECHANICAL ENGINEERING)

Approved by,



(Ir. Idris bin Ibrahim)

**Idris bin Ibrahim, P.Eng. MNEM**  
Senior Lecturer  
Mechanical Engineering Department  
Universiti Teknologi PETRONAS

UNIVERSITI TEKNOLOGI PETRONAS

TRONOH, PERAK

MAY 2011

## CERTIFICATION OF ORIGINALITY

This is to certify that I am responsible for the work submitted in this project, that the original work is my own except as specified in the references and acknowledgements, and that the original work contained herein have not been undertaken or done by unspecified sources or persons.

---

MOHD SYAFIQRUL IKHWAN BIN MOHD ZULKIFLI

## ABSTRACT

A stable Vertical Take-off and Landing Operation (VTOL) capability is very important for Micro Unmanned Aerial Vehicle (MUAV). It will enable the aircraft to conduct operation in such difficult situations. To achieve that, it becomes a main priority to have a suitable and good control system to control the stability of the MUAV's body during take-off and landing operations. The objectives of this project are to study possible methods of controlling the MUAV's VTOL operations, the quad rotor dynamic modeling concept of the MUAV as well as the control allocation for the MUAV's VTOL system. After that, the modeling and simulation processes will be conducted to the selected control allocation. As a first step, the literature review stage which covers the studies from various sources is done to get a proper idea regarding the MUAV and VTOL operation. The modeling and control allocation study is conducted to study the method in conducting modeling processes and control allocation involved for the control system. Along the process, the design methodology has been discussed along with an iterative algorithm derived. All the data, parameters and formulas have been validated during the data analysis and validation stage. After all of information have been gathered and validated, the control system has been modeled and simulated during the final stage of the project. In this stage also, all the characteristics and parameters have been adjusted and perfected to get the desired results. As for the results, the final control system is consist of a set of sensors that will give reading in x, y and z-coordinates. Besides, the self-programmable Microchip pic18f4431 processor also has been selected which the control system coding can be embedded. The selected microchip has the onboard high-speed analog digital (A/D) converter and the power pulse width modulation (PWM) module. The module on the microchip will convert the analog signal from the sensors to the digital signal so that it can be read by the motor driver. The motor driver will equally distribute and balance the power to all four of the MUAV's motors so that it can ensure the MUAV's body remains stable during take-off and landing operations.

## ACKNOWLEDGMENT

First of all, the author would like to express utmost gratitude and appreciation to Allah because with His blessings and help, the Final Year Project went very smoothly. Alhamdulillah, all praises to Him that the author have been able to complete this project on time.

This project would not have been possible without the assistance and guidance of certain individuals and organization whose contributions have helped in its completion. First and foremost, the author would like to express his sincere thanks and utmost appreciation to the project supervisor, Ir. Idris Bin Ibrahim for having faith and strong support in guiding the author throughout the whole period of completing the final year project. His kind assistance and guidance from the beginning to the end of this study really help me to undergo my project successfully.

Special express gratitude is also reserved for the Mechanical Engineering Department of Universiti Teknologi PETRONAS for providing excellent support in terms of providing cutting edge knowledge and information not just within the Final Year Project but also the five years spent undergoing every single bit of invaluable knowledge on mechanical engineering.

The author would also like to deliver his warmth appreciation to the post graduate students who are involved with this project, namely Mr. Tamiru Alemu and Ms. Diyana Firyana for assisting with the technical support and guidance towards this project.

Finally many thanks to the author's family and fellow colleagues for their help and ideas throughout the completion of this study. I hope that the outcome of this report will bring beneficial output to others as well. Thank you very much everyone.

## TABLE OF CONTENTS

<b>CERTIFICATION OF APPROVAL</b>	. . . . .	<b>ii</b>
<b>CERTIFICATION OF ORIGINALITY</b>	. . . . .	<b>iii</b>
<b>ABSTRACT</b>	. . . . .	<b>iv</b>
<b>ACKNOWLEDGEMENT</b>	. . . . .	<b>v</b>
<b>TABLE OF CONTENTS</b>	. . . . .	<b>vi</b>
<b>LIST OF FIGURES</b>	. . . . .	<b>viii</b>
<b>LIST OF TABLES</b>	. . . . .	<b>ix</b>
<b>CHAPTER 1:</b>	<b>INTRODUCTION</b>	<b>1</b>
	1.1 Project Background	1
	1.2 Problem Statement	2
	1.3 Objective	3
	1.4 Scope of Study.	3
<b>CHAPTER 2:</b>	<b>LITERATURE REVIEW</b>	<b>5</b>
	2.1 Flight Dynamics	5
	2.2 Rotorcraft	7
	2.3 Quad rotor	7
	2.4 Quad Rotor Design Overview.	12
	2.5 VTOL System.	14
	2.6 Pulse Width Modulation (PWM)	16
	2.7 Proportional Integral Derivative (PID) Controller	19

<b>CHAPTER 3:</b>	<b>METHODOLOGY</b>	<b>27</b>
3.1	Project Flowchart	27
3.2	Software and Hardware Requirement.	29
<b>CHAPTER 4:</b>	<b>RESULTS AND DISCUSSIONS</b>	<b>31</b>
4.1	VTOL Controls System Overview	31
4.1.1	Control System Schematic	32
4.1.2	Sensors	33
4.1.3	Controller	33
4.1.4	Circuit	34
4.2	Dynamic Modeling and Simulation	35
4.2.1	Dynamics of Quad rotor	35
4.2.2	System of Differential Equations	36
4.2.3	PID Controller Design	38
4.2.4	PID Controller Results and Simulation	39
4.2.5	Motor Power Variation Effect on MUAV Body Simulations	42
<b>CHAPTER 5:</b>	<b>CONCLUSIONS &amp; RECOMMENDATIONS</b>	<b>46</b>
5.1	Conclusion.	46
5.2	Recommendations	47
<b>REFERENCES</b>		<b>48</b>
<b>APPENDICES</b>		<b>52</b>
A1	Project Milestone for Final Year I	52
A2	Project Milestone for Final Year II	53
A3	Circuit Diagrams	54
A4	Simulation Code	60

## LIST OF FIGURES

Figure 2.1	Body-fixed coordinate system . . . . .	5
Figure 2.2	Airplane Reference Axes . . . . .	6
Figure 2.3	Quad rotor unmanned aerial vehicle motion control . . . . .	8
Figure 2.4	Simplified quad rotor in hovering . . . . .	9
Figure 2.5	Throttle movement of quad rotor . . . . .	9
Figure 2.6	Roll movement of quad rotor . . . . .	10
Figure 2.7	Pitch movement of quad rotor. . . . .	10
Figure 2.8	Yaw movement of quad rotor . . . . .	11
Figure 2.9	3D model of the physical structure of the Quad rotor . . . . .	12
Figure 2.10	The Curtiss-Wright X-19 VTOL Aircraft . . . . .	14
Figure 2.11	Quad rotor aircraft. Thrust Vectoring Mechanism . . . . .	15
Figure 2.12	PWM signals of varying duty cycles . . . . .	17
Figure 2.13	A simple PWM circuit . . . . .	17
Figure 2.14	Conventional feedback control system . . . . .	19
Figure 2.15	Simple mass, spring and damper model . . . . .	21
Figure 2.16	Open loop state response graph . . . . .	22
Figure 2.17	Proportional control example graph . . . . .	23
Figure 2.18	Proportional - derivative example graph . . . . .	24
Figure 2.19	Proportional - derivative example graph . . . . .	25
Figure 2.20	Proportional – integral - derivative example graphs . . . . .	26
Figure 3.1	Research Methodology Flow Chart . . . . .	27
Figure 4.1	Control System Schematic . . . . .	31
Figure 4.2	Rate Integrating Gyroscope . . . . .	32
Figure 4.3	Dual- axis Accelerometer . . . . .	32
Figure 4.4	Ultrasonic Sensor . . . . .	32
Figure 4.5	3D Quad Rotor model. . . . .	35
Figure 4.6	Quad-Rotor Schematic . . . . .	36
Figure 4.7	The final simulation model with the PID controllers for the quad rotor . . . . .	40
Figure 4.8	Plot drawing represent the z-axis moving to the desired z-point . . . . .	40



Figure 4.9	Plot drawing represents the Phi (Roll) angle after 3 seconds to start moving to the desired point . . . . .	41
Figure 4.10	Plot drawing represents the Psi (Yaw) angle after 5 seconds to start moving to the desired point . . . . .	41
Figure 4.11	Plot drawing represents the Theta (Pitch) angle start moving to the desired point . . . . .	41
Figure 4.12	First MATLAB simulation results . . . . .	44
Figure 4.13	Second MATLAB simulation results . . . . .	44
Figure 4.14	Third MATLAB simulation results . . . . .	45
Figure A1	Project Milestone for Final Year I . . . . .	52
Figure A2	Project Milestone for Final Year II . . . . .	53
Figure A3	Circuit Diagrams . . . . .	54

#### LIST OF TABLES

Table 2.1	Rotorcraft features comparison . . . . .	11
Table 2.2	Quad rotor main structural components . . . . .	12
Table 2.3	Summary of effects of each PID controller . . . . .	20
Table 3.1	Software Requirement . . . . .	29
Table 3.2	Hardware Requirement . . . . .	30
Table 4.1	Physical parameters used in MATLAB analysis . . . . .	43
Table 4.2	Predicted moment of inertia . . . . .	43
Table 4.3	Initial conditions used to solve equations in MATLAB Simulation . . . . .	43

# CHAPTER 1

## INTRODUCTION

### 1.1 Project Background

#### 1.1.1 Unmanned Aviation (UV)

Unmanned aviation had its beginnings with the model built and flown by Cayley, Stringfellow, Du Temple, and other aviation pioneers as precursors to their attempts at manned flight in the first half of the nineteenth century. These models were used as the technology testbeds for larger, man-carrying versions, and in this sense they were forerunners of manned aviation (Newcome, 2004).

#### 1.1.2 Unmanned Aerial Vehicle (UAV)

An unmanned aerial vehicle (UAV) is an aircraft that flies without a human crew on board the aircraft. The term UAV came into general use in the early 1990s to describe robotic and replaced the term remotely piloted vehicle (RPV) which was used during the Vietnam War and afterward.

UAV has various applications but it is widely used in military applications. UAV falls into five functional categories which are:

- **Target and decoy** - providing ground and aerial gunnery a target that simulates an enemy aircraft or missile
- **Reconnaissance** - providing battlefield intelligence
- **Combat** - providing attack capability for high-risk missions Logistics - UAVs specifically designed for cargo and logistics operation
- **Research and development** - used to further develop UAV technologies to be integrated into field deployed UAV aircraft
- **Civil and Commercial UAVs** - UAVs specifically designed for civil and commercial applications. (The UAV, 2010).

There are a wide variety of UAV shapes, sizes, configurations, and characteristics. The earliest unmanned aerial vehicle was A. M. Low's "Aerial Target" of 1916 (Monash, 2010). In constructing the UAV, it demands a vast knowledge of base vehicle platforms, flight dynamics, control theory, and real time software in a network environment.

### **1.1.3 Vertical Take-Off and Landing (VTOL)**

The VTOL system is a system that enables the aircraft to take-off and landing vertically with power rotor. The common example of VTOL system can be seen on helicopter. Meanwhile, autogyros, balloons, airships and rockets are not normally considered VTOL aircraft, but may be termed VTVL (Vertical Takeoff with Vertical Landing).

The applications of VTOL system can simply being beneficial to the aircrafts. It will enable the aircraft to take-off and landing in such a compact area. In term of cost-saving, the aircraft companies will be saving in constructing the long and paved runaways. The VTOL system also will enable the aircraft to operate in the difficult conditions.

## **1.2 Problem Statement**

The VTOL capability is very crucial in operation of Micro Unmanned Aerial Vehicle (MUAV). It will enable the aircraft to conduct operation in such difficult situations and have potential for fulfilling many civil and military applications. To achieve that, the VTOL operation must have a stable take-off and landing operation.

The problem encountered by the most VTOL MUAV is the instability of MUAV's body during take-off and landing operation. It is caused by many factors such as the environment of the MUAV's operation take place (wind, geographical factors), the unstable power distribution from MUAV's motor and also the error reading by the MUAV's sensors. This problem will cause the MUAV to settle unsteadily on air after take-off operation and it is also possible to cause the MUAV to crash on the ground if the landing operation cannot be conducted properly.

To deal with this problem, it becomes a main priority to have a suitable and good control system to control the stability of the MUAV's body during take-off and landing operations. This control system will include a set of sensors, a programmable microcontroller, and the control coding that control the whole MUAV's VTOL operation. This control system will read the reading by the sensors, convert the analog signal from the sensors to the digital signal to enable the motor controller to read it and lastly distribute the power equally to all MUAV's motors to maintain the stability of MUAV's body.

To find the best control system that can control the stability of the MUAV's body during VTOL operation is a major challenge in this project. A lot of dynamic modelling and mathematical equations have to be analyzed. There are also a lot of considerations have to be taken into account such as the MUAV's body design, the rotor system that is going to be used and the environment that the MUAV's operation will take place.

### **1.3 Objectives**

These are the project objectives:

- To study possible methods of controlling the MUAV's VTOL operations.
- To study the quad rotor dynamic modeling concept of the MUAV
- To study the control allocation for the MUAV's VTOL system.
- To conduct the modeling and simulation processes to the selected control allocation.

### **1.4 Scope of Study**

The project is done to study the best control system for MUAV's VTOL system. This control system will maintain the stability of MUAV body during take-off and landing operations.

This project basically includes the study of the possible control system for the MUAV's VTOL operation. It will cover the study of the dynamic modeling of the quad-rotor system as well as the control allocation for the take-off and landing operation of the MUAV. Besides, the project also will cover the

modelling and simulating processes of the control system using MATLAB and any other related software. The output of this project is expected to be the control system's block diagram, mathematical model of the control system and the analysis result from MATLAB and any other software as well as the basic control system architecture for the MUAV application.

## CHAPTER 2

### LITERATURE REVIEW

#### 2.1 Flight Dynamics

The first step towards dynamic modeling of an airplane is to consider it as a rigid body with six degrees of freedom (DOF), followed by application of Newton's laws to the rigid body (airplane).

Figure 2.1 depicts the body-fixed reference frame (moving frame) that is attached to the airplane. The center  $C$  of the body-fixed reference frame  $Cxyz$  coincides with the center of gravity (CG) of the airplane. The  $Cxz$  plane coincides with the plane of symmetry of the airplane with the  $Cx$  and  $Cz$  axes pointing forward and downward, respectively. The  $Cy$  axis is perpendicular to the plane of symmetry in the direction of the right wing. The  $Cxyz$  body-fixed reference frame is a right-handed Cartesian coordinate system.

The linear velocity components of the CG along the  $Cx$ ,  $Cy$  and  $Cz$  axes are defined as  $U$ ,  $V$  and  $W$ , respectively. The angular velocity components about the axes of the body-fixed reference frame are defined as  $P$ ,  $Q$  and  $R$ , respectively.

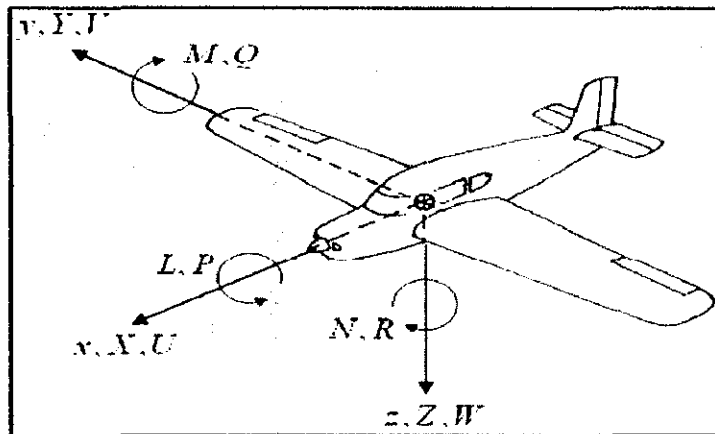


Figure 2.1: Body-fixed coordinate system.

External aerodynamic forces components along the axes are denoted by  $X$ ,  $Y$  and  $Z$ . The components about the axes of the external aerodynamic moments are denoted by  $L$ ,  $M$  and  $N$ . (Valvanis, 2006, p.51)

According to Robert F. Stengel (2004), flight dynamics is the science of air and space vehicle orientation and control in three dimensions. The three critical flight dynamics parameters are the angles of rotation in three dimensions about the vehicle's centre of mass, known as pitch, roll and yaw.

- Pitch - Angle of X Body Axis (nose) relative to horizon. Also a positive (nose up) rotation about Y Body Axis
- Roll - Angle of Y Body Axis (wing) relative to horizon. Also a positive (right wing down) rotation about X Body Axis
- Yaw - Angle of X Body Axis (nose) relative to North. Also a positive (nose right) rotation about Z Body axis

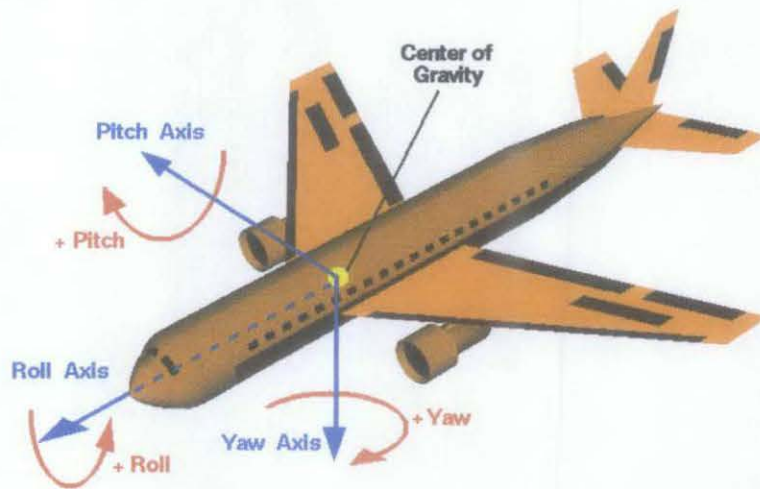


Figure 2.2: Airplane Reference Axes (Robert F. Stengel, 2004)

The determination of these three axes helps the aerospace engineers in designing the control system of the aircraft. The control system will operate about the aircraft's centre of mass, it include actuator which will exert forces in various directions, and generate rotational forces or moments about the aerodynamic centre of the aircraft, and thus rotate the aircraft in pitch, roll, or yaw.

Based on Jan Roskam (2001), each and every aircraft must abide to the general flights characteristic such as:

- The airplanes must have sufficient control power to maintain steady state, straight line flight throughout the design flight envelope.

- It must be possible for the airplane to be safely maneuvered from one steady state flight condition to another.

As a conclusion, the determining of the three major flights dynamic's parameters will results in the good control system which will be able to meet the basic characteristics outlined for every aircraft.

## 2.2 Rotorcraft

From the previous research project by Hidayah (2009), the MUAV will be using rotorcraft as the lifting mechanism.

Based on her study also, she defines,

Rotorcraft is a heavier-than-air flying machine that uses lift generated by wings, called rotor blades that revolve around a mast. Several rotor blades mounted to a single mast are referred to as a rotor.

A rotorcraft may have one or more rotors. Various rotor configurations have been used such as:

- **Single rotor** - One rotor disc.
- **Twin rotor** - Two rotor discs. These usually rotate in opposite directions, so that no tail rotor or other yaw stabiliser is needed:
- **Tandem** - One in front of the other.
- **Transverse** - Side by side.
- **Coaxial** - One rotor disc above the other, with concentric drive shafts.
- More than two rotor discs: in the case of one at each corner giving a quad rotor.

## 2.3 Quad Rotor

A quad rotor is a four-rotor helicopter. It is an under-actuated, dynamic vehicle with four input forces and six degrees of freedom. Unlike regular helicopters that have variable pitch angle rotors, a quad rotor helicopter has four fixed-pitch angle rotors.

The basic motions of a quad rotor are generated by varying the rotor speeds of all four rotors, thereby changing the lift forces. The helicopter tilts



towards the direction of the slow spinning rotor, which enables acceleration along that direction. Therefore, control of the tilt angles and the motion of the helicopter are closely related and estimation of orientation (roll and pitch) is critical. Spinning directions of the rotors are set to balance the moments and eliminate the need for a tail rotor. This principle is also used to produce the desired yaw motions. (Kivrak, 2006, p.17)

Based on Hoffman, Huang, Waslander and Tomlin (2007, p.1) quad rotor operates when there are four rotors, two pairs are counter-rotating, fixed pitch-blades located at the four corners of the aircraft.

Quad rotor generates its motion by only controlling the angular velocity of each rotor as shown in the Figure 2.3 below:

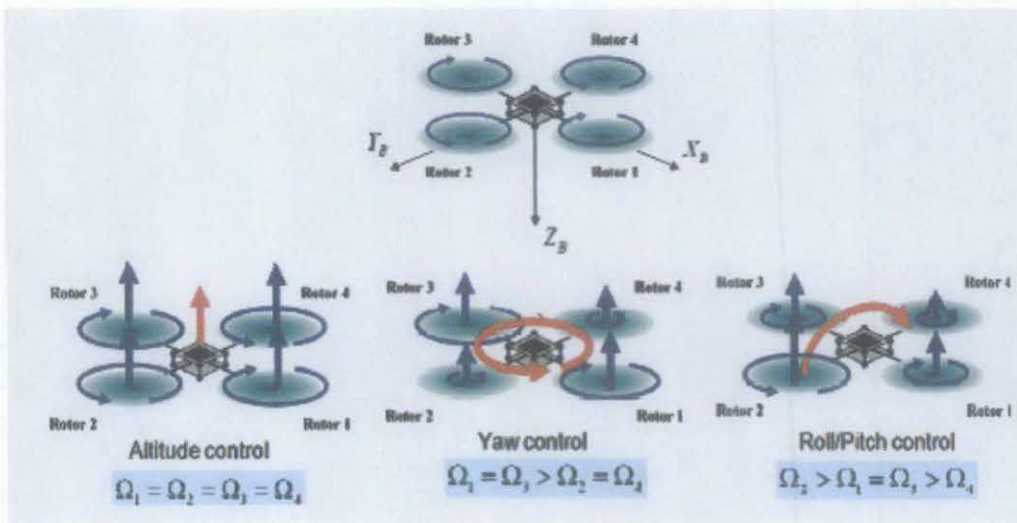


Figure 2.3: Quad-rotor unmanned aerial vehicle motion control

(Hyondong Oh, Dae-Yeon Won, Sung-Sik Huh, David Hyunchul Shim and Min-Jea Tahk (2010) p.72)

In the Figure 2.3 above,  $\Omega$  represents the angular velocity. In order to avoid the yaw drift due to the reactive torques, rotors 1 and 3 rotate clockwise, and rotors 2 and 4 rotate counter-clockwise. Altitude control is achieved by changing the total thrust while maintaining equal individual thrusts. Moreover, yaw motion is made by reducing the thrust of one set of rotors and increasing the thrust of the other set while maintaining the same total thrust. On the other hand, roll and pitch motion is achieved by increasing one rotor's thrust and

decreasing the other rotor's thrust. (Hyondong Oh, Dae-Yeon Won, Sung-Sik Huh, David Hyunchul Shim and Min-Jea Tahk, 2010, p.72)

The detail explanations on the various motion concepts of the quad rotor are as below. Figure 2.4 shows the simplified quad rotor operation in the hovering state:

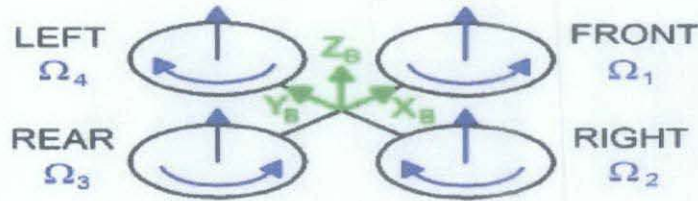


Figure 2.4: Simplified quad rotor in hovering (Bresciani, 2008, p.22)

### 2.3.1 Throttling

If the weight of the quad rotor is distributed symmetrically as well as its geometry, changing all the rotor speed at the same amount will produce vertical movement which rises or lowered the quad rotor. This command used when taking off or landing the quad rotor. Figure 2.5 shows the throttling command on the quad rotor. The movement is in the  $\ddot{z}$  direction.

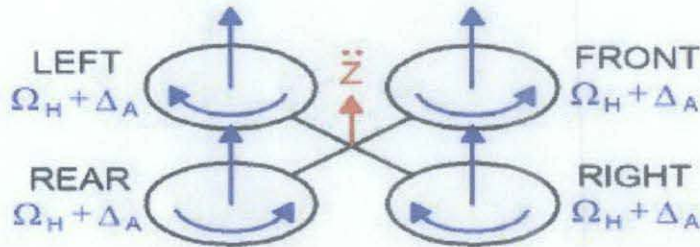


Figure 2.5: Throttle movement of quad rotor (Bresciani, 2008, p.23)

### 2.3.2 Roll

Roll movements makes quad rotor to turn with respect to the roll axis rotating about the centre of gravity (NASA 2008). By increasing or decreasing the left propeller speed and by decreasing or increasing the rights one, the torque will make it turn. Rear and front rotor will be maintained in speed to balance the lift. The angle of roll denoted by  $\phi$  angle called roll angle as shown in Figure 2.6.

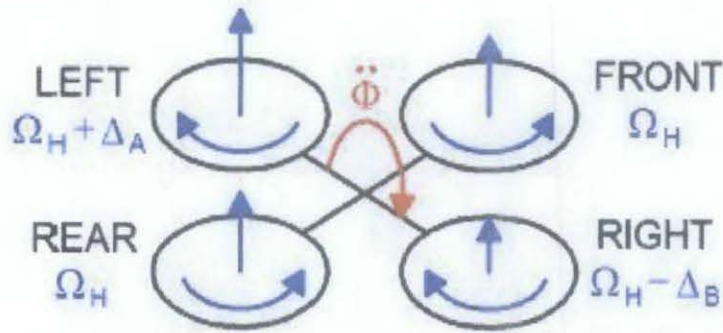


Figure 2.6: Roll movement of quad rotor (Bresciani, 2008, p.24)

### 2.3.3 Pitch

This command is very similar to the roll and is provided by increasing or the rear propeller speed and by decreasing the front one or vice versa. Pitching the quad rotor means tilting up or down the rotorcraft with respect to the pitch axis led by the torque produced. The pitch axis is perpendicular to the aircraft centreline and lies in the plane of the wings (NASA, 2008). Figure 2.7 shows the pitch movement of the quad rotor. The amount of pitching is given by pitch angle  $\ddot{\theta}$ .

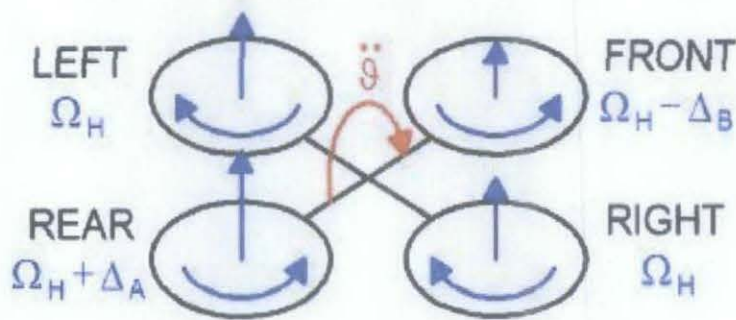


Figure 2.7: Pitch movement of quad rotor (Bresciani, 2008, p.25)

### 2.3.4 Yaw

The yaw movement is generated from the fact that the left-right rotors rotate clockwise while the front-rear rotors rotate counter-clockwise. Hence, when the overall torque is unbalanced, the helicopter turns on itself around yaw axis. Yaw provided by increasing the front-rear rotor speed and by decreasing that of the left-right couple or vice versa. It leads to a torque with respect to the yaw axis which makes the quad rotor turn (NASA, 2008). Yaw

motion represented in Figure 2.8 shows the movement of the quad rotor in turning by its side.

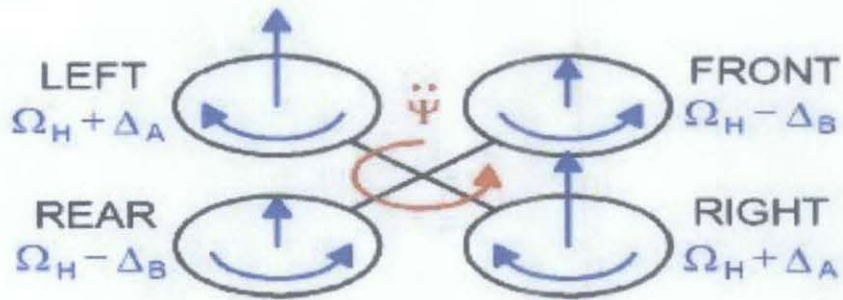


Figure 2.8: Yaw movement of quad rotor (Bresciani, 2008, p.25)

The quad rotor system also is the best system for the VTOL operation. Based on the comparison from various features between quad rotor system with other type of rotor systems. Table 2.1 clearly shows that the quad rotor system is the best system to be applied for the VTOL manipulations.

Table 2.1: Rotorcraft features comparison as 1=Worse and 4=Best (Hidayah, 2009)

	A	B	C	D	E	F	G	H
Power cost	2	2	2	2	1	4	3	3
Control cost	1	1	4	2	3	3	2	1
Payload/volume	2	2	4	3	3	1	2	1
Maneuverability	4	2	2	3	3	1	3	3
Mechanics simplicity	1	3	3	1	4	4	1	1
Aerodynamics complexity	1	1	1	1	4	3	1	1
Low speed flight	4	3	4	3	4	4	2	2
High speed flight	2	4	1	2	3	1	3	3
Miniaturization	2	3	4	2	3	1	2	4
Survivability	1	3	3	1	1	3	2	3
Stationary flight	4	4	4	4	4	3	1	2
<b>Total</b>	<b>24</b>	<b>28</b>	<b>32</b>	<b>24</b>	<b>33</b>	<b>28</b>	<b>22</b>	<b>24</b>

A=Single rotor, B=Axial rotor, C=Coaxial rotors, D=Tandem rotors, E=Quadrotor, F=Blimp, G=Bird-like, H=Insect-like.

## 2.4 Quad Rotor Design Overview



Figure 2.9: 3D model of the physical structure of the Quadrotor (Canetta, Chin, Mehrabian, Montejo, Thompson, 2007, p.1)

The following Table 2.2 summarizes the main structural components of the quad-rotor craft design.

Table 2.2: Quad Rotor main structural components

Quantity	Part Name
1	Central Hub
4	Arm
4	Motor Mount
4	DC Motor
4	Gear Box
2	Pusher Propeller
2	Tractor Propeller

### 2.4.1 Motors

The motors are cobalt, brushed, DC motors rated for 12 V, 15 amps. The DC, brushed motor configuration was desired for ease of control (ability to control via PWM). The cobalt motors use strong rare earth magnets and provide the best power to weight ratio of the hobby motors available for model aircraft.

## **2.4.2 Propellers**

The propellers are 10" from tip to tip. Two are of the tractor style, for clockwise rotation, and the other two are of the pusher style, for counterclockwise rotation. A propeller with a shallow angle of attack was necessary as it provided the vertical lift for stable hovering.

## **2.4.3 Gearboxes**

The gearboxes have a 2.5:1 gear ratio. They reduce the speed of the prop compared to the speed of the motor, allowing the motors to exert more torque on the propellers while drawing much less current than in a direct drive configuration.

## **2.4.4 Arms**

The arms of our quad-rotor design needed to be light and strong enough to withstand the stress and strain caused by the weight of the motors and the central hub at their opposite ends. Carbon fiber was deemed the best choice because of its weight to strength ratio. The thickness of the tube was chosen to be the smallest possible to lower its weight. The length of each arm was chosen based on the propellers. The propellers' length has to allow enough room for them to spin without encountering turbulence from one another.

## **2.4.5 Battery**

The battery was selected on the basis of power requirements for the selected motor/gearbox combination.

## **2.4.6 Hub**

The central hub carries all of the electronics, sensors, and battery. It sits lower than the four motors in order to bring the center of gravity downwards for increased stability.

## **2.4.7 Motor Mounts**

The motor mounts connect the motors to the carbon fiber arms.

## 2.5 VTOL System

### 2.5.1 VTOL overview

VTOL is a flight technique in which an aircraft rises directly into the air and settles vertically onto the ground (Answers.com, 2010). This classification includes only a very few aircraft; helicopters, gyrocopters, autogyros, gyroplanes, balloons and airships are not considered VTOL. Some aircraft can operate in VTOL mode in addition to others, such as CTOL (Conventional Take-off and Landing). Others can only operate by VTOL, due to the aircraft lacking landing gear that can handle horizontal motion (Wordiq.com, 2010)

According to (Tesla, 1993, p.273)

VTOL system was first patented by Serbian physicist and electrical engineer, and inventor of the radio and the electric motor and generator, Nikola Tesla on January 3, 1928. It described a method of achieved vertical take-off, transition to and from horizontal flight, and vertical landing, with a tilting rotor

There are many aircraft that used VTOL system nowadays, among that is Curtiss-Wright X-19. In X-19, the idea is using a propeller's radial lift to generate the lift required to fly at low forward speeds and up through transition. The prop not only would propel the aircraft forward, but also would provide lift during forward flight. This would free the aircraft from having a wing sized for low speed flight.



Figure 2.10: The Curtiss-Wright X-19 VTOL Aircraft  
([www.456fis.org/CURTISS\\_WRIGHT\\_X-19.htm](http://www.456fis.org/CURTISS_WRIGHT_X-19.htm), 2010)

## 2.5.2 Thrust Vectoring

Thrust vectoring, also thrust vector control or TVC, is the ability of an aircraft, rocket or other vehicle to manipulate the direction of the thrust from its engine(s) or motor in order to control the attitude or angular velocity of the vehicle.

For aircraft, the method was originally envisaged to provide upward vertical thrust as a means to give aircraft vertical (VTOL) landing ability. Subsequently, it was realized that using vectored thrust in combat situations enabled aircraft to perform various maneuvers not available to conventional-engine planes. To perform turns, aircraft that use no thrust vectoring must rely on only aerodynamic control surfaces, such as ailerons or elevator craft with vectoring must still use control surfaces, but to a lesser extent.

Most currently operational vectored thrust aircraft use turbofans with rotating nozzles or vanes to deflect the exhaust stream. This method can successfully deflect thrust through as much as 90 degrees, relative to the aircraft centreline. However, the engine must be sized for vertical lift, rather than normal flight, which results in a weight penalty (Hubfaces, 2006)

As for the quad rotor aircraft, under consideration consists of a rigid cross frame equipped with four rotors as shown in Fig. 2.11. The up (down) motion is achieved by increasing (decreasing) the total thrust while maintaining an equal individual thrust. The forward/backward, left/right and the yaw motions are achieved through a differential control strategy of the thrust generated by each rotor. (Tayebi, McGilvray, 2006, p.562-563)

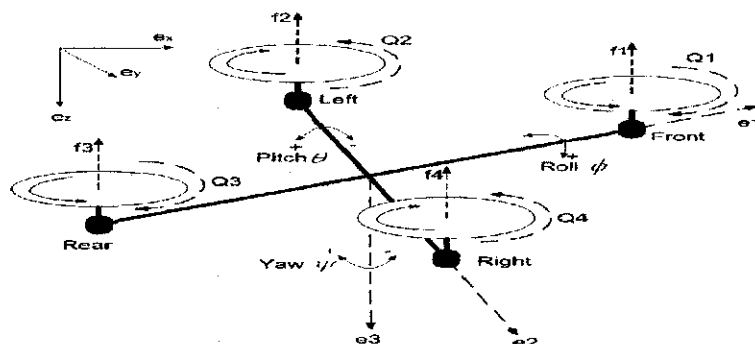


Figure 2.11: Quadrotor aircraft. Thrust Vectoring Mechanism (Tayebi, McGilvray, 2006, p.563)



## **2.6 Pulse Width Modulation (PWM)**

Pulse width modulation (PWM) is a powerful technique for controlling analog circuits with a processor's digital outputs. PWM is employed in a wide variety of applications, ranging from measurement and communications to power control and conversion.

### **2.6.1 Analog electronics**

An analog signal has a continuously varying value, with infinite resolution in both time and magnitude. A nine-volt battery is an example of an analog device, in that its output voltage is not precisely 9V, changes over time, and can take any real-numbered value. Similarly, the amount of current drawn from a battery is not limited to a finite set of possible values. Analog signals are distinguishable from digital signals because the latter always take values only from a finite set of predetermined possibilities, such as the set {0V, 5V}.

### **2.6.2 Digital control**

By controlling analog circuits digitally, system costs and power consumption can be drastically reduced. What's more, many microcontrollers and DSPs already include on-chip PWM controllers, making implementation easy.

PWM is a way of digitally encoding analog signal levels. Through the use of high-resolution counters, the duty cycle of a square wave is modulated to encode a specific analog signal level. The PWM signal is still digital because, at any given instant of time, the full DC supply is either fully on or fully off. The voltage or current source is supplied to the analog load by means of a repeating series of on and off pulses. The on-time is the time during which the DC supply is applied to the load, and the off-time is the periods during which that supply is switched off. Given a sufficient bandwidth, any analog value can be encoded with PWM.

Figure 2.12 shows three different PWM signals. Figure 2.12a shows a PWM output at a 10% duty cycle. That is, the signal is on for 10% of the period and off the other 90%. Figures 2.12b and 2.12c show PWM output at

50% and 90% duty cycles, respectively. These three PWM outputs encode three different analog signal values, at 10%, 50%, and 90% of the full strength. If, for example, the supply is 9V and the duty cycle is 10%, a 0.9V analog signal results

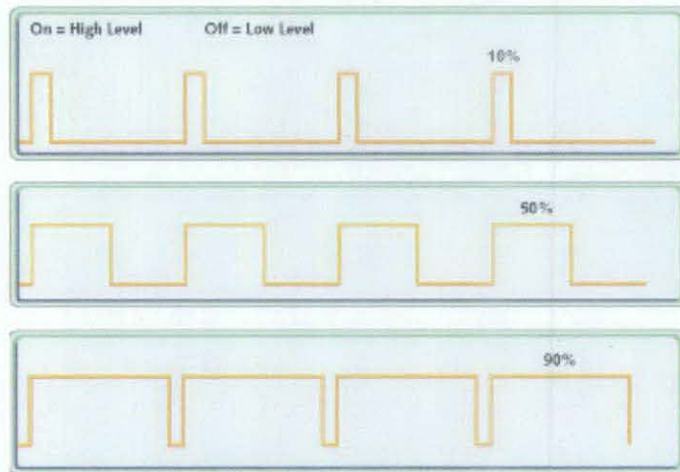


Figure 2.12(from top to bottom) a,b,c : PWM signals of varying duty cycles (Introduction to Pulse Width Modulation (PWM), 2011)

Figure 2.13 shows a simple circuit that could be driven using PWM. In the figure, a 9 V battery powers an incandescent light bulb. If we closed the switch connecting the battery and lamp for 50 ms, the bulb would receive 9 V during that interval. If we then opened the switch for the next 50 ms, the bulb would receive 0 V. If we repeat this cycle 10 times a second, the bulb will be lit as though it were connected to a 4.5 V battery (50% of 9 V). We say that the duty cycle is 50% and the modulating frequency is 10 Hz.

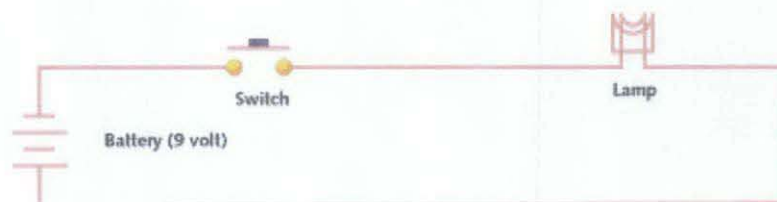


Figure 2.13: A simple PWM circuit ((Introduction to Pulse Width Modulation (PWM), 2011)

### 2.6.3 PWM controllers

Many microcontrollers include on-chip PWM controllers. The duty cycle is the ratio of the on-time to the period; the modulating frequency is the inverse of the period. To start PWM operation, the data sheet suggests the software should:

- Set the period in the on-chip timer/counter that provides the modulating square wave
- Set the on-time in the PWM control register
- Set the direction of the PWM output, which is one of the general-purpose I/O pins
- Start the timer
- Enable the PWM controller

Although specific PWM controllers do vary in their programmatic details, the basic idea is generally the same.

### 2.6.4 Advantages of the PWM

- The signal remains digital all the way from the processor to the controlled system; no digital-to-analog conversion is necessary. By keeping the signal digital, noise effects are minimized. Noise can only affect a digital signal if it is strong enough to change a logic-1 to a logic-0, or vice versa.
- PWM finds application in a variety of systems. As a concrete example, a PWM-controlled brake.
- PWM is economical, space saving, and noise immune.

((Introduction to Pulse Width Modulation (PWM), 2011)

### 2.7 Proportional Integral Derivative (PID) Controller

The PID controller, which consists of proportional, integral and derivative elements, is widely used in feedback control of industrial processes. It is a controller that includes elements with those three functions. The PID

controller was first placed on the market in 1939 and has remained the most widely used controller in process control until today.

PID control is the method of feedback control that uses the PID controller as the main tool. The basic structure of conventional feedback control systems is shown in Figure 2.14, using a block diagram representation. In this figure, the process is the object to be controlled. The purpose of control is to make the process variable  $y$  follow the set-point value  $r$ . To achieve this purpose, the manipulated variable  $u$  is changed at the command of the controller. As an example of processes, consider a heating tank in which some liquid is heated to a desired temperature by burning fuel gas. The process variable  $y$  is the temperature of the liquid, and the manipulated variable  $u$  is the flow of the fuel gas.

The disturbance is any factor, other than the manipulated variable, that influences the process variable. Figure 2.14 assumes that only one disturbance is added to the manipulated variable. In some applications, however, a major disturbance enters the process in a different way, or plural disturbances need to be considered. The error  $e$  is defined by  $e = r - y$ . The compensator  $C(s)$  is the computational rule that determines the manipulated variable  $u$  based on its input data, which is the error  $e$  in the case of Figure 2.14. The last thing to notice about Figure 2.14 is that the process variable  $y$  is assumed to be measured by the detector, which is not shown explicitly here, with sufficient accuracy instantaneously that the input to the controller can be regarded as being exactly equal to  $y$ .

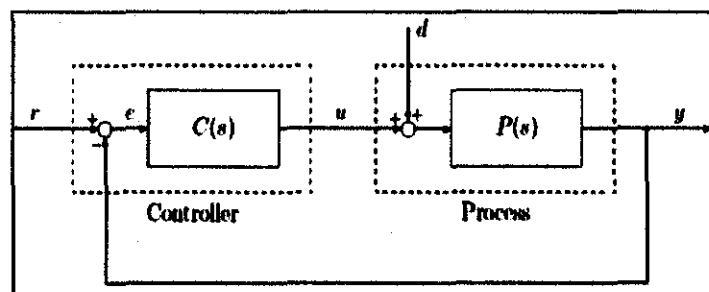


Figure 2.14: Conventional feedback control system (PID Tutorial, 1997)

Early PID control systems had exactly the structure of Figure 2.14, where the PID controller is used as the compensator  $C(s)$ . When used in this way, the three elements of the PID controller produce outputs with the following nature:

- P element: proportional to the error at the instant  $t$ , which is the present error
- I element: proportional to the integral of the error up to the instant  $t$ , which can be interpreted as the accumulation of the past error.
- D element: proportional to the derivative of the error at the instant  $t$ , which can be interpreted as the prediction of the future error.

(Araki, 2011)

### 2.7.1 The characteristics of P, I, and D controllers

A proportional controller ( $K_p$ ) will have the effect of reducing the rise time and will reduce, but never eliminate, the steady-state error. An integral control ( $K_i$ ) will have the effect of eliminating the steady-state error, but it may make the transient response worse. A derivative control ( $K_d$ ) will have the effect of increasing the stability of the system, reducing the overshoot, and improving the transient response. Effects of each of controllers  $K_p$ ,  $K_d$ , and  $K_i$  on a closed-loop system are summarized in the table shown below.

Table 2.3: Summary of effects of each PID controller (PID Tutorial, 1997)

CL RESPONSE	RISE TIME	OVERSHOOT	SETTLING TIME	S-S ERROR
<b>K<sub>p</sub></b>	Decrease	Increase	Small Change	Decrease
<b>K<sub>i</sub></b>	Decrease	Increase	Increase	Eliminate
<b>K<sub>d</sub></b>	Small Change	Decrease	Decrease	Small Change

Suppose we have a simple mass, spring, and damper problem as shown in the figure below:

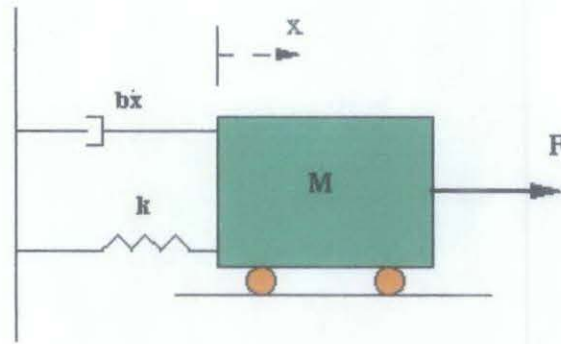


Figure 2.15: Simple mass, spring and damper model (PID Tutorial, 1997)

The modeling equation of this system is

$$M\ddot{x} + b\dot{x} + kx = F \quad (2.1)$$

Taking the Laplace transform of the modeling equation 2.1

$$Ms^2X(s) + bsX(s) + kX(s) = F(s) \quad (2.2)$$

The transfer function between the displacement  $X(s)$  and the input  $F(s)$  then becomes

$$\frac{X(s)}{F(s)} = \frac{1}{Ms^2 + bs + k} \quad (2.3)$$

Let

- $M = 1\text{kg}$
- $b = 10\text{ N.s/m}$
- $k = 20\text{ N/m}$
- $F(s) = 1$

Plug these values into the above transfer function

$$\frac{X(s)}{F(s)} = \frac{1}{s^2 + 10s + 20} \quad (2.4)$$

The goal of this problem is to show you how each of  $K_p$ ,  $K_i$  and  $K_d$  contributes to obtain

- Fast rise time
- Minimum overshoot
- No steady-state error

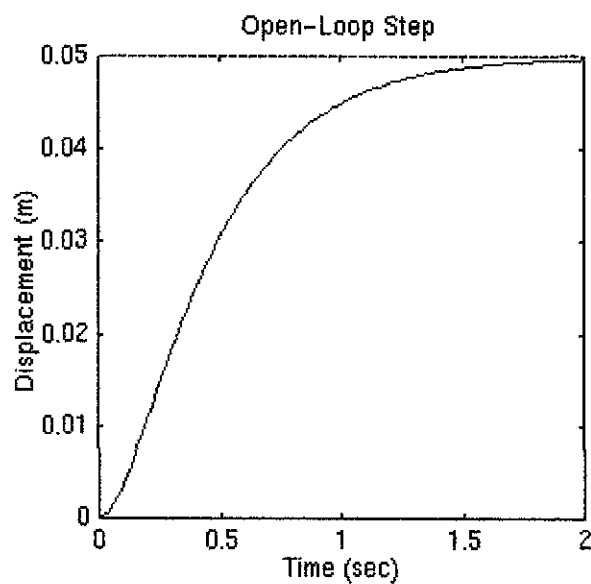


Figure 2.16: Open loop state response graph (PID Tutorial, 1997)

The DC gain of the plant transfer function is  $1/20$ , so 0.05 is the final value of the output to an unit step input. This corresponds to the steady-state error of 0.95, quite large indeed. Furthermore, the rise time is about one second, and the settling time is about 1.5 seconds

### **Proportional (P) control**

From the table shown above, the proportional controller ( $K_p$ ) is capable to reduces the rise time, increases the overshoot, and reduces the steady-state error. The closed-loop transfer function of the above system with a proportional controller is:

$$\frac{X(s)}{F(s)} = \frac{K_p}{s^2 + 10s + (20 + K_p)} \quad (2.5)$$

If the proportional gain ( $K_p$ ) equals 300 and the following graph will be plotted:

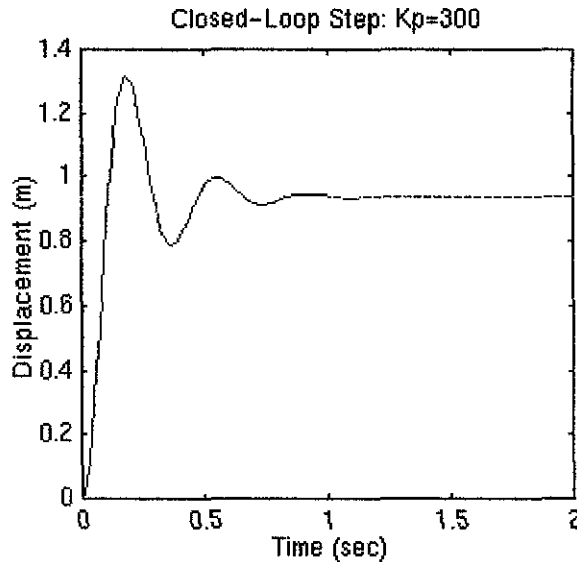


Figure 2.17: Proportional control example graph (PID Tutorial, 1997)

The above plot shows that the proportional controller reduced both the rise time and the steady-state error, increased the overshoot, and decreased the settling time by small amount.

### Proportional-Derivative (PD) control

For the PD control, as the table shown above, the derivative controller ( $K_d$ ) can reduce both the overshoot and the settling time. The closed-loop transfer function of the given system with a PD controller is:

$$\frac{X(s)}{F(s)} = \frac{K_D s + K_p}{s^2 + (10 + K_D)s + (20 + K_p)} \quad (2.6)$$

Let  $K_p$  equals to 300 as before and let  $K_d$  equals 10. The following graph will be yielded:



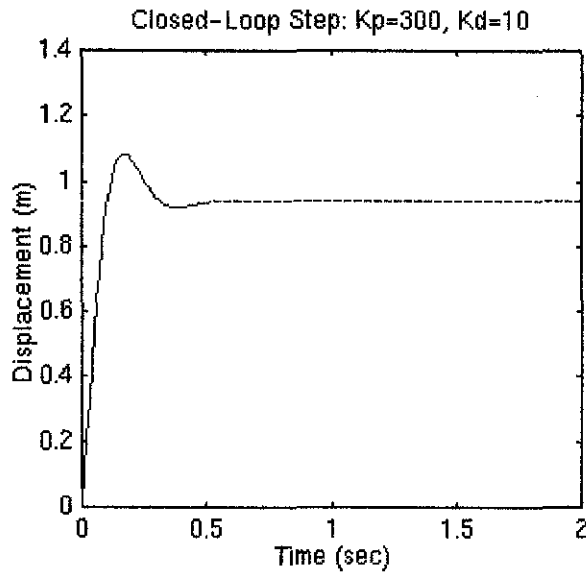


Figure 2.18: Proportional - derivative example graph (PID Tutorial, 1997)

This plot shows that the derivative controller reduced both the overshoot and the settling time, and had small effect on the rise time and the steady-state error.

### **Proportional-Integral (PI) control**

From the table, integral controller ( $K_i$ ) can decrease the rise time, increase both the overshoot and the settling time, and eliminate the steady-state error. For the given system, the closed-loop transfer function with a PI control is:

$$\frac{X(s)}{F(s)} = \frac{K_p s + K_i}{s^2 + 10s^2 + (20 + K_p)s + K_i} \quad (2.7)$$

The  $K_p$  value is set to 30, and  $K_i$  equals to 70.

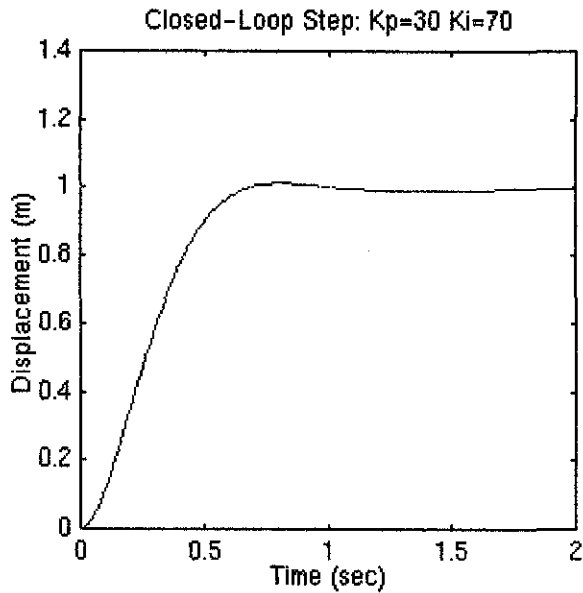


Figure 2.19: Proportional - derivative example graph (PID Tutorial, 1997)

The above response shows that the integral controller eliminated the steady-state error.

### Proportional-Integral-Derivative (PID) control

As for PID controller, the closed-loop transfer function of the given system with a PID controller is:

$$\frac{X(s)}{F(s)} = \frac{K_D s^2 + K_P s + K_I}{s^3 + (10 + K_D)s^2 + (20 + K_P)s + K_I} \quad (2.8)$$

The value is set with  $K_P=350$ ,  $K_I=300$ , and  $K_D=50$  so that it can provided the desired response.

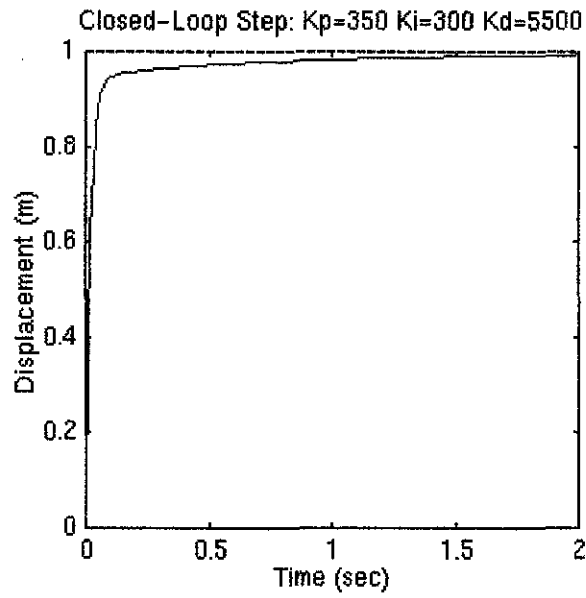


Figure 2.20: Proportional – integral - derivative example graph (PID Tutorial, 1997)

The system obtained has no overshoot, fast rise time, and no steady-state error.

(PID Tutorial, 1997)

# CHAPTER 3

## METHODOLOGY/PROJECT WORK

### 3.1 Project Flowchart

The flow chart below shows the research project methodology. The Gantt charts of the project planning for FYP I and II are attached in **Appendix A1 and A2**.

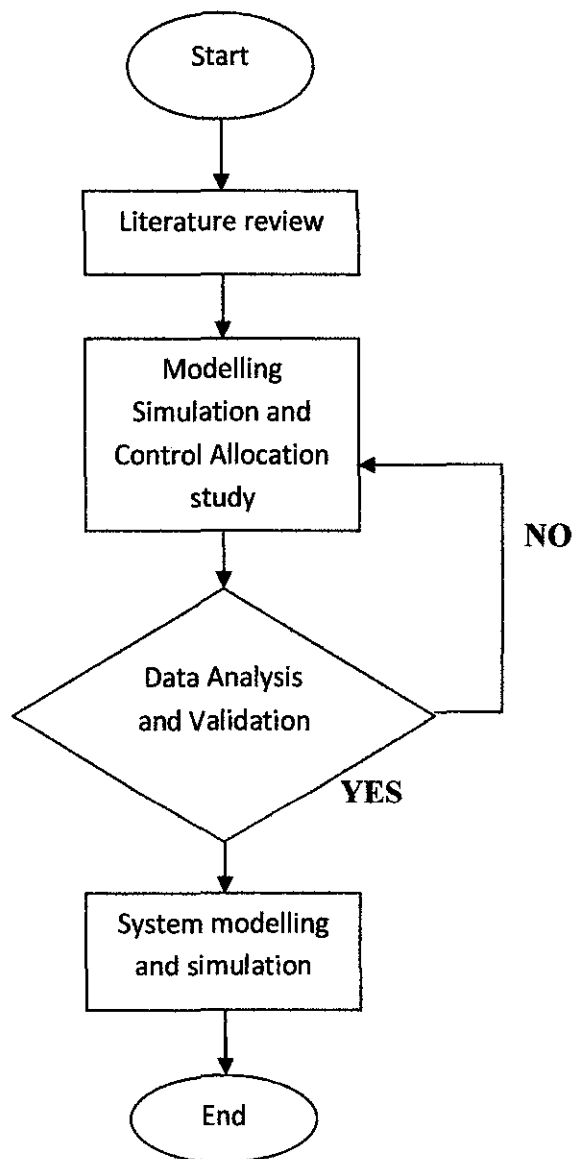


Figure 3.1: Research Methodology Flow Chart

### **3.1.1 Literature Review**

During this stage, the studies will be carried out from various sources such as journals, books, and websites that are related to the UAV's control system. These studies will cover the VTOL system that used in most of the UAV. It also will cover the possible control system that can be used to control the VTOL of the MUAUV. The data gathered through these studies will be used to get develop the initial concept of the control system for the MUAUV's VTOL system

### **3.1.2 Modelling and Control Allocation Study**

At this stage of study, the control system studies will be focusing on the method to conduct modelling processes and control allocation involved for the control system. Along the process, the design methodology will be discussed along with an iterative algorithm derived. All the parameters and formulas that been discovered at this stage will be very useful for the system modeling and simulation stage later.

### **3.1.3 Data Analysis and Validation**

The data analysis and validation stage will be performed once all the control system parameters and formulas have been gathered from the early stage. During this stage, all the formulas will be elaborateg with the suitable parameters. From the equations, the basic control block diagram will be sketched. From this stage, the early image of the control system architecture can be visualised.

### **3.1.4 System Modelling and Simulation**

From the initial control system architecture developed from the research, the model of the control system will be built up and developrd. The calculations that formed will be justified using the MATLAB software. From the calculations, the control structure and block diagram of the control system will be structured and we will get a clear theoretical view on the operation of the control system.

The simulation process otherwise is a continuation from the modelling process. Once the model was developed, all the calculations formula will be simulated. From the simulation process, all the parameters in the equations will be simulated in the graph form or any related figures. From this process also, the characteristics that can be adjusted and perfected will be determined in order to get the desired result. The modelling and simulating the control system will be carried out using MATLAB software and any related software necessary.

### 3.2 Software and Hardware Requirement

#### 3.2.1 Software Requirement

The Table 3.1 below shows the list of software that is essential in running this research project:

Table 3.1: Software Requirement

<b>Software</b>	<b>Model</b>	<b>Reason</b>
Operating system	Microsoft Windows XP Professional OS Service Pack 2	To operate the computer's system
Supporting software	MatlabR2009b	-Matrix manipulations -Plotting of functions and data -Implementation of algorithms
Supporting software	Autocad 2009	For 2D and 3D design and drafting
Supporting software	Simulink	Modeling, simulating and analyzing multidomain dynamic systems
Supporting software	Visual Basic 2008	To develop the Control System Guest User Interface (GUI)

### 3.2.2 Hardware Requirement

The Table 3.2 below shows the list of hardware that is essential in running this research project:

Table 3.2: Hardware Requirement

Hardware	Model	Reason
Central Processor Unit (CPU)	AMD Athlon 64, 2200 MHz (11 x 200) 3500+	- Fast and reliable processor - Compatible with software used
Main Memory	1792 MB (DDR2-800 DDR2 Random Access Memory (RAM))	Allow stored data to be accessed in any order at random
Motherboard	Abit A-N68SV (2 PCI, 1 PCI-E x1, 1 PCI-E x16, 2 DDR2 DIMM, Audio, Video, LAN)	Central circuit board of the computer. Relay information between all the components in the computer
Motherboard Chipset	nVIDIA nForce 7025-630a, AMD Hammer	To manage data throughput
Graphic Card	NVIDIA GeForce 7025 / NVIDIA nForce 630a (512 MB)	Allows fast transfer of information
Hard Disk	Hitachi HDT725025VLA380 (250 GB, 7200 RPM, SATA-II)	Non-volatile storage device for digital data
Monitor	AOC 831W 19" LCD Plug and Play Monitor [NoDB] (1825233121)	To displays images or symbols generated by computers

## CHAPTER 4

### RESULTS AND DISCUSSION

#### 4.1 VTOL Controls System Overview

##### 4.1.1 Control System Schematic

The following schematic in Figure 4.1 depicts the MUAV controls system. The diagram represents how the control system interacts with the physical system for controlled quad-rotor flight.

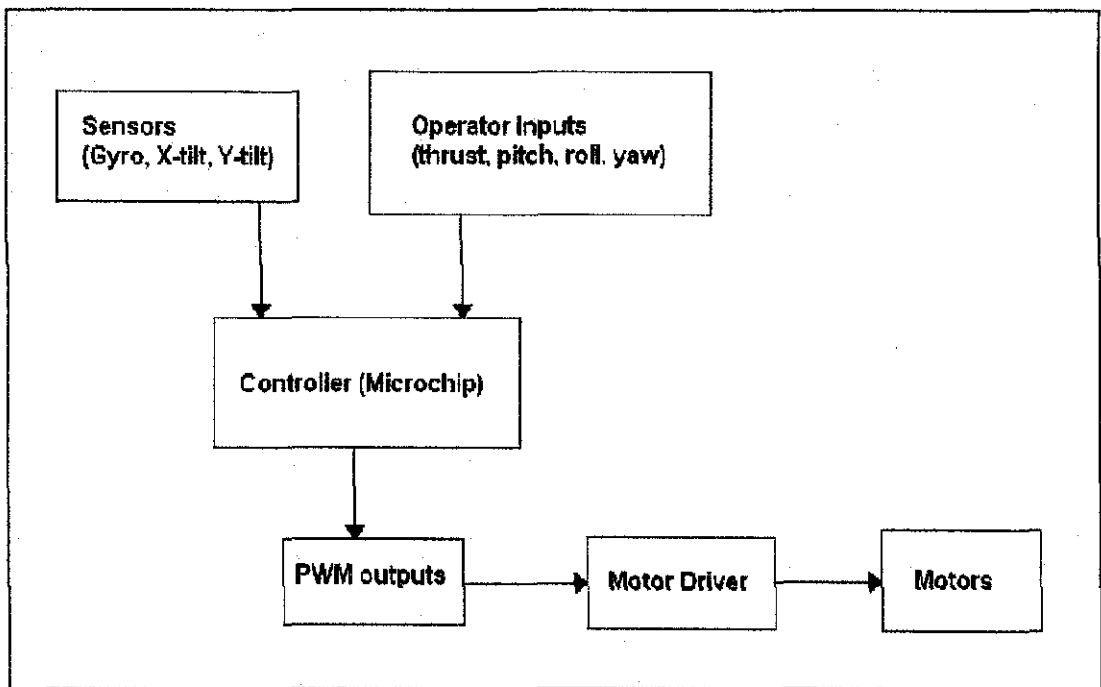


Figure 4.1: Control System Schematic



## 4.1.2 Sensors

### 4.1.2.1 Gyroscope

A single-axis gyroscope in the center of the craft in order to measure the yaw rate while in flight.

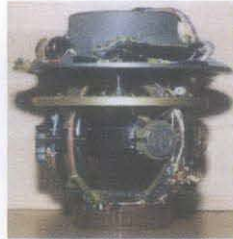


Figure 4.2: Rate Integrating Gyroscope

### 4.1.2.2 XY Accelerometer

The dual-axis accelerometer (tilt sensors) located on the central hub of the craft. These tilt sensors each provided X- and Y- analog output signals. The outputs from the two sensors were averaged for higher sensitivity.



Figure 4.3: Dual- axis Accelerometer

### 4.1.2.3 Ultrasonic (UT) Sensor

UT Sensors being located on the central hub and it measures altitude of the MUAV (provide a stable altitude control)



Figure 4.4: Ultrasonic Sensor

### 4.1.3 Controller

The Microchip microcomputer acted as the controller for the system. A proportional, closed-loop control system was chosen for its simplicity, both in implementation and function, as well as its effectiveness.

Since such a system was chosen, the sole feedback for the system is proportional to the error, or the difference between the command and the output, as read by the onboard sensors. This error is then amplified by a gain so as to adjust the sensitivity of the control system.

Ultimately, such a control system was implemented by taking advantage of two particular modules on the **Microchip pic18f4431** processor: the onboard high-speed A/D converter and the power pulse width modulation (PWM) module.

The A/D converter is used to measure seven analog signals; four command signals representing overall thrust, roll, pitch, and yaw, and four onboard sensors, which monitor the tilt along two axes, the yaw rotation of the entire body as well as the altitude of the aircraft. This data is then interpolated by the processor to calculate the error. This error is then amplified by a fixed gain, and since the hypothetical responses of the dynamics of the vehicle are known, new output signals are then calculated and outputted to the four motors via the PWM module using the following equations:

- $outMotorA = (kThrust*(inThrust) - (kElevator*(inElevator-512) + kTiltX*(inTiltX-512)) - (kRudder*(inRudder-512) + kGyroZ*(inGyroZ-512)))$  (4.1)
- $outMotorB = (kThrust*(inThrust) + (kAilerons*(inAilerons-512) + kTiltY*(inTiltY-512)) + (kRudder*(inRudder-512) + kGyroZ*(inGyroZ-512)))$  (4.2)
- $outMotorC = (kThrust*(inThrust) - (kAilerons*(inAilerons-512) + kTiltY*(inTiltY-512)) + (kRudder*(inRudder-512) + kGyroZ*(inGyroZ-512)))$  (4.3)

- $outMotorD = (kThrust*(inThrust) + (kElevator*(inElevator-512) - kTiltX*(inTiltX-512)) - (kRudder*(inRudder-512) + kGyroZ*(inGyroZ-512)))$  (4.4)

These equations factor in seven gains (represented by the variable names beginning with “k”) corresponding to their respective inputs, as well as the fact that for all of the sensors and inputs, except for thrust, the values allow for both positive and negative variation from the rest value. There also exists a fail-safe where the level of thrust for a particular motor never falls below a given limit. This fail-safe prevents the motors, which require a fair amount of power to start from idle, from stalling in mid-air. The C-Code for Proportional Control System shows in **Appendix A4**. The end result is a microcontroller which not only enables the MUA V to fly, but provides stability in doing so.

#### 4.1.4 Circuit

The schematics for the circuits used are provided in **Appendix A3**. Namely, they detail the circuit used to amplify the sensor signals and send them to the microcomputer, as well as the circuit used to amplify the PWM outputs in order to drive the motor. There are also schematics for the individual connections made to each of the sensors and the microcomputer.

## 4.2 Dynamic Modeling and Simulation

### 4.2.1 Dynamics of Quad rotor

In order to move the quad rotor model from the earth to a fixed point in the space, the mathematical design should depend on the direction cosine matrix as Equation 4.5. A body fixed frame is assumed to be at the center of gravity of the quad rotor, where the z-axis is pointing upwards. This body axis is related to the inertial frame by a position vector  $(x,y,z)$  and 3 Euler angles,  $(\theta,\phi,\psi)$ , representing pitch, roll and yaw respectively. A ZYX-Euler angle representation given in Equation 4.5 has been chosen for the representation of the rotations.

$$R = \begin{pmatrix} c_\phi c_\theta & c_\phi s_\theta s_\psi - s_\phi c_\psi & c_\phi s_\theta c_\psi + s_\phi s_\psi \\ s_\phi c_\theta & s_\phi s_\theta s_\psi + c_\phi c_\psi & s_\phi s_\theta c_\psi - c_\phi s_\psi \\ -s_\theta & c_\theta s_\psi & c_\theta c_\psi \end{pmatrix} \quad (4.5)$$

where  $c_\theta$  and  $s_\theta$  represent  $\cos \theta$  and  $\sin \theta$  respectively.

Each rotor produces moments as well as vertical forces. These moments have been experimentally observed to be linearly dependent on the forces for low speeds. There are four input forces and six output states  $(x, y, z, \theta, \psi, \phi)$  therefore the quad rotor is an under-actuated system. The rotation direction of two of the rotors are clockwise while the other two are counterclockwise, in order to balance the moments and produce yaw motions as needed. The Figure 4.5 below shows the 3D Quad Rotor which represents the Euler angles and forces acting on the quad rotor body.

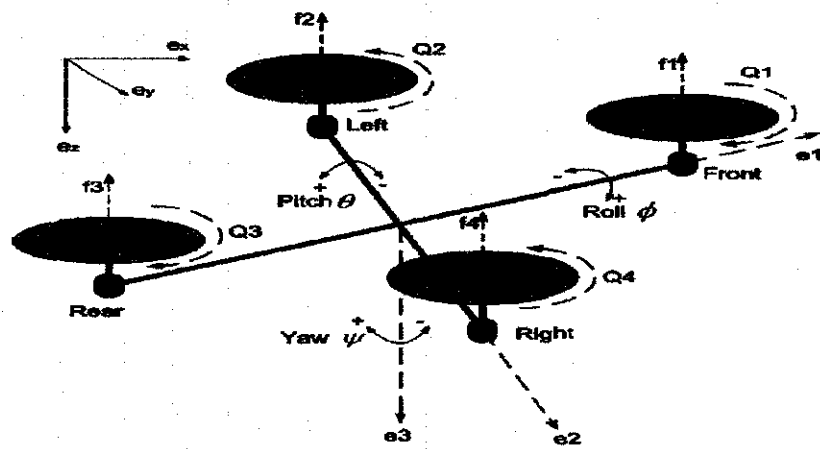


Figure 4.5: 3D Quad Rotor model

#### 4.2.2 System of Differential Equations

The dynamics of the quad-rotor UAV are determined from a set of equations of motion. The complexity of the equations of motion increases with increased accuracy.

The set of equations presented model the motion of the craft based on the amount of lift delivered by each individual motor without taking into account the aerodynamics of the craft.

Figure 4.6 is a top-down view of the craft. Motion is obtained by varying the amount of lift each motor provides. The amount of lift each motor provides is controlled by the amount of power delivered to each motor. Depending on the motor and gearbox used, the relationship can be linear, parabolic, or a combination of various other trigonometric functions.

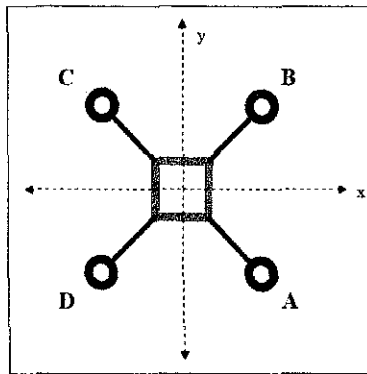


Figure 4.6: Quad-Rotor Schematic

For example, the craft will move in the positive x-direction by reducing the thrust from motor A (by reducing the power) and simultaneously increasing the thrust (by increasing the power) from motor C. The thrust from motor B and D must be increased so that the craft maintains constant altitude while moving along the desired path. More complex movements can be achieved by varying the power delivered to all four motor.

Based on the Lagrange approach (Altud, 2002), the equations of motion that govern the dynamics of the craft are listed below:

$$\left. \begin{aligned} \ddot{x} &= u_1 (\cos \phi \sin \theta \cos \psi + \sin \phi \sin \psi) - K_1 \dot{x} / m \\ \ddot{y} &= u_1 (\sin \phi \sin \psi \cos \psi - \cos \phi \sin \psi) - K_2 \dot{y} / m \\ \ddot{z} &= u_1 (\cos \phi \cos \psi) - g - K_3 \dot{z} / m \end{aligned} \right\} \quad (4.6)$$

Where:

x: Forward position in earth axes

y: Lateral position in earth axes

z: Vertical position in earth axes

Ki: The Drag Coefficients for the system.

The Ki's given above are the drag coefficient and it assume to be zero, since drag is negligible at low speeds. The center of gravity is assumed to be at the middle of the connecting link

As the center of gravity moves up (or down) d units, then the angular acceleration becomes less sensitive to the forces, therefore stability is increased. Stability can also be increased by tilting the rotor forces towards the center. This will decrease the roll and pitch moments as well as the total vertical thrust and it is given by:

$$\left. \begin{aligned} U_1 &= (Th_1 + Th_2 + Th_3 + Th_4) / m \\ U_2 &= l(-Th_1 - Th_2 + Th_3 + Th_4) / I_1 \\ U_3 &= l(-Th_1 + Th_2 + Th_3 - Th_4) / I_2 \\ U_4 &= C(Th_1 + Th_2 + Th_3 + Th_4) / I_4 \end{aligned} \right\} \quad (4.7)$$

Where:

U<sub>1</sub>: Vertical thrust generated by the four rotors

U<sub>2</sub>: Pitching moment

U<sub>3</sub>: Yawing moment

U<sub>4</sub>: Rolling moment

Th<sub>i</sub>: The thrusts generated by four rotors

I<sub>i</sub>: The moments of inertia with respect to the axes

m: total mass of the helicopter;

$l$ : half length of the helicopter

Therefore the equations of Euler angles become:

$$\left. \begin{aligned} \ddot{\theta} &= u_2 - lK_4 \dot{\theta} / I_1 \\ \ddot{\psi} &= u_3 - lK_5 \dot{\psi} / I_2 \\ \ddot{\phi} &= u_4 - K_6 \dot{\phi} / I_3 \end{aligned} \right\} \quad (4.8)$$

Where  $\theta$ ,  $\phi$ , and  $\psi$  are three Euler angles, representing pitch, roll and yaw respectively.

### 4.2.3 PID Controller Design

The literature review of the PID controller has been explained in Chapter 2. As for the MUAV quad rotor, the PID controller is developed based on the fast response. Using this approach as a recursive algorithm for the control-laws synthesis, all the calculation stages concerning the tracking errors are simplified.

One other aspect of the controller selection depends on the method of control of the MUAV. It can be mode-based or non-mode based. For the mode based controller, independent controllers for each state are needed, and a higher level controller decides how these interact. On the other hand for a non-mode based controller, a single controller controls all of the states together. However the adopted control strategy is summarized in the control of two subsystems; the first relates to the position control while the second is that of the attitude control. The quad rotor model can be divided into two subsystems:

- A fully-actuated subsystem that provides the dynamics of the vertical position  $z$  and the yaw angle ( $z$  and  $\psi$ ).

$$\begin{bmatrix} \ddot{z} \\ \ddot{\phi} \end{bmatrix} = \begin{bmatrix} u_1 \cos\phi \cos\psi - g \\ u_4 \end{bmatrix} + \begin{bmatrix} -K_3 \dot{z} / m \\ -K_6 \dot{\phi} / I_3 \end{bmatrix} \quad (4.9)$$

- An under actuated subsystem representing the under actuated subsystem which gives the dynamic relation of the horizontal positions (x, y) with the pitch and roll angles.

$$\begin{bmatrix} \ddot{x} \\ \ddot{y} \end{bmatrix} = \begin{bmatrix} u_1 \cos\phi & u_1 \sin\phi \\ u_1 \sin\phi & -u_1 \cos\phi \end{bmatrix} \begin{bmatrix} \sin\theta \cos\psi \\ \sin\psi \end{bmatrix} + \begin{bmatrix} -K_1 \dot{x}/m \\ -K_2 \dot{y}/m \end{bmatrix} \quad (4.10)$$

and,

$$\begin{bmatrix} \ddot{\theta} \\ \ddot{\psi} \end{bmatrix} = \begin{bmatrix} u_2 \\ u_3 \end{bmatrix} + \begin{bmatrix} -IK_4 \dot{\theta}/I_1 \\ -IK_5 \dot{\psi}/I_2 \end{bmatrix} \quad (4.11)$$

Since drag is very small at low speeds, the drag terms in the above equations can be considered as small disturbances to the system. The PID control is applied to the equations above with inputs  $u_1, u_2, u_3, u_4$  and outputs  $\phi, \theta, \psi$  and  $Z_d$ .

#### 4.2.4 PID Controller Results and Simulation

The nominal parameters and the initial conditions of the quad rotor for simulation are:

$$I_1=I_2=1.25 \text{ Ns}^2/\text{rad}.$$

$$I_3=2.5 \text{ Ns}^2/\text{rad}.$$

$$K_1=K_2=K_3=0.010 \text{ Ns/m}.$$

$$K_4=K_5=K_6=0.012 \text{ Ns/rad}.$$

$$m=2 \text{ kg. } l=0.2 \text{ m. } g=9.8 \text{ m/s}^2.$$

the proposed control algorithm shown in Figure 4.7 ,which is composed of all controllers, inputs, speed reference and the inner relationships of the thrust , the quad rotor system is supplied by a step function for the altitude and (z-axis) which is subject to the three step inputs at (3,10 ,20) and the response yields as can be seen in Figure 4.8 which is contains some transient overshoot and another for the Yaw angle ( $\psi$ ) which is subjected to step input after 5 second as shown in Figure 4.9 and the roll angle ( $\phi$ ) which is respond after 3 second as it can be seen in Figure 4.10,the pitch angle response is shown in Figure 4.11 which 5% overshoot



when subjected to step input .these transient perturbation are due to many reasons such as an certain of some mechanical parameters in the design and the simplification of controller design .

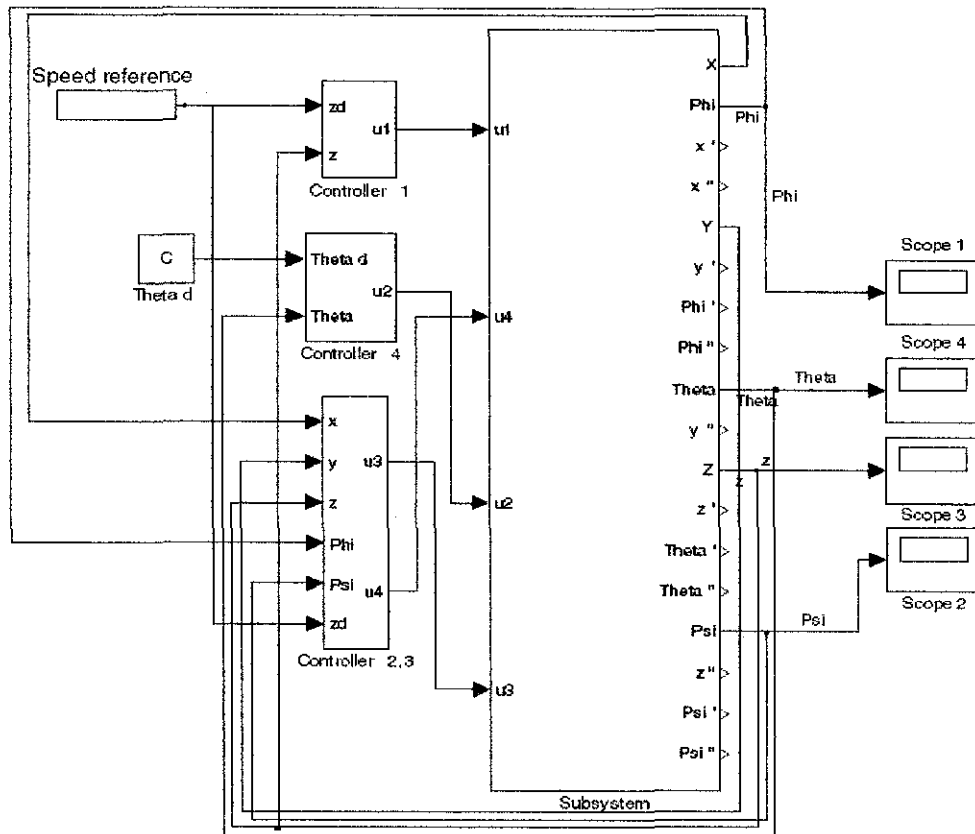


Figure 4.7: The final simulation model with the PID controllers for the quad rotor

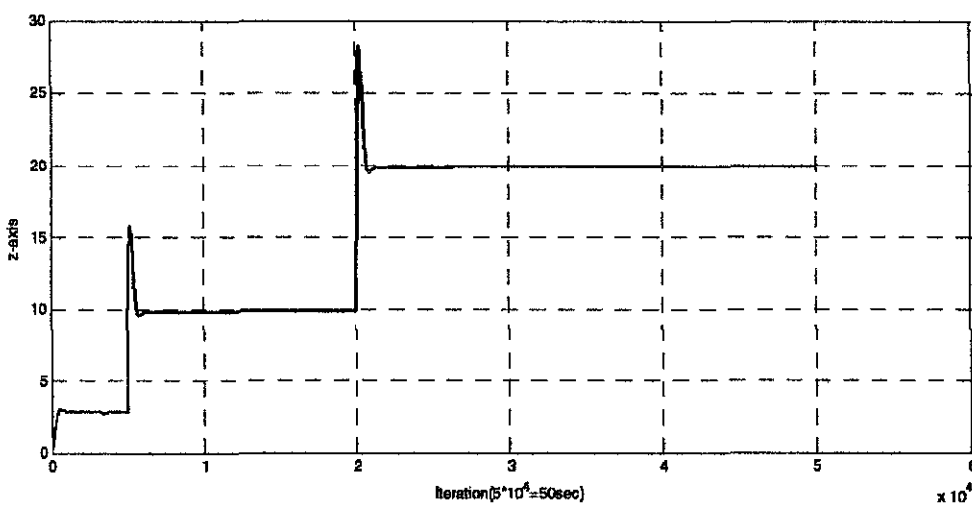


Figure 4.8: Plot drawing represent the z-axis moving to the desired z-point

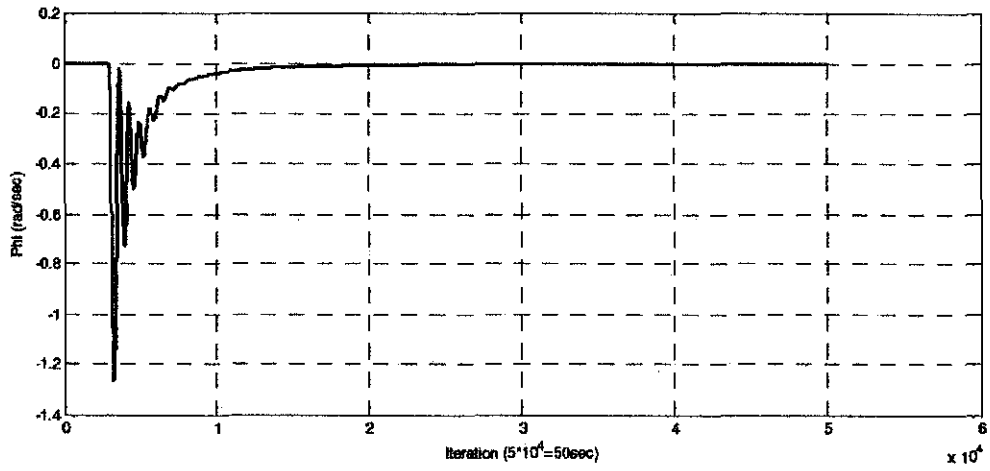


Figure 4.9: Plot drawing represent the Phi (Roll) angle after 3 seconds to start moving to the desired point

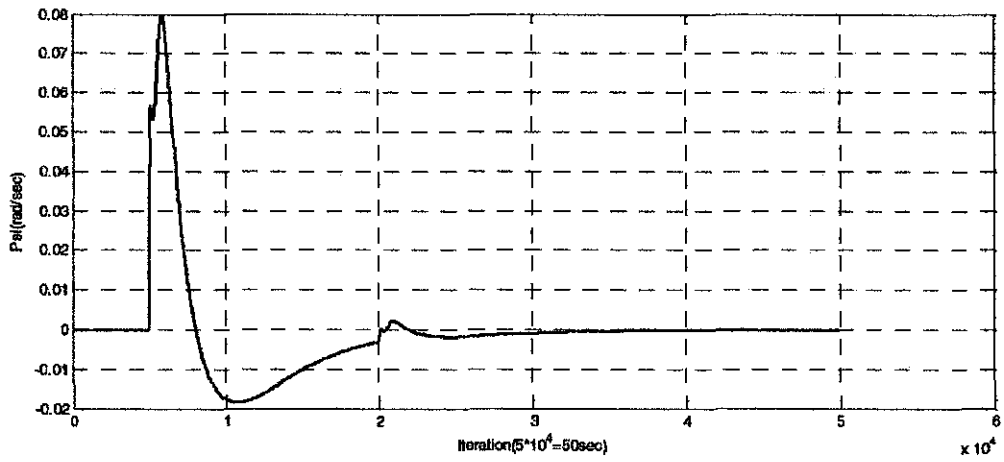


Figure 4.10: Plot drawing represent the Psi (Yaw) angle after 5 seconds to start moving to the desired point

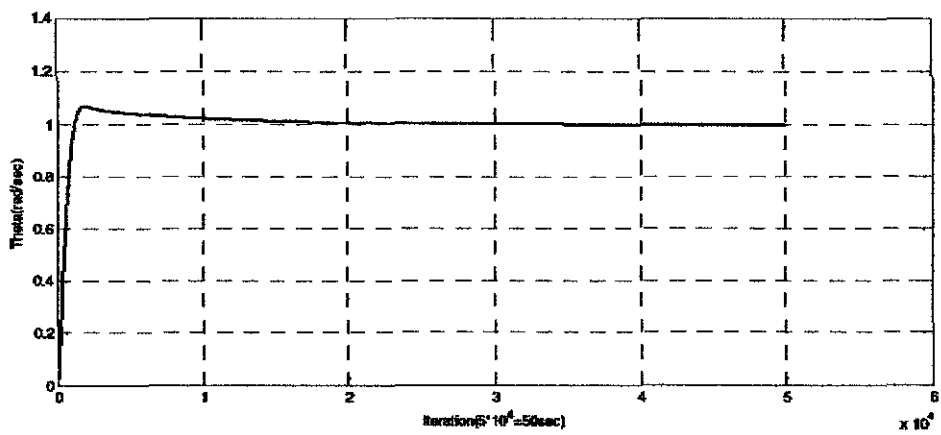


Figure 4.11: Plot drawing represent the Theta (Pitch) angle start moving to the desired point

The simulation results show that the PID controllers are able to robustly stabilize the quad rotor helicopter and move it to a desired position with a desired yaw angle while keeping the pitch and the roll angles zero. The design also is easy and has a fast response time. The PID controllers used to control  $z$ , which is sensitive to the changes for the other parameters. The good performance can be shown from the speed of response of the quad rotor; although the overshoot in the altitude response was removed, the transient response of the system became faster. The same speed of response can be also seen in the yaw, pitch and roll angles control of Figure 4.8, 4.9 and 4.10.

#### **4.2.5 Motor Power Variation Effect on MUAUV Body Simulations**

The craft can increase in altitude by simultaneously increasing the thrust from all motors. Likewise, the craft can descend (if already airborne) by simultaneously decreasing the thrust from all motors.

The MATLAB software is used to solve the system of six differential equations that simulate the craft's motion. To solve the equations, the package ODE45 program is used. Please see **Appendix A4** to see the two sets of code that solves the system.

Simulations were performed to ensure the validity of the basic assumptions about the behavior of the craft when power is varied to the motors. When possible, the basic parameters were estimated. Parameters that could not be estimated without a detailed study of the craft and the air around it were estimated to unity.

The moments of inertia were determined by modeling the central hub as a square, the motors as cylinders, and the propellers as rods. The parallel axis theorem applied to sum the moments of inertia due to each individual motor. Table 4.1 summarizes the parameters used in these calculations. Table 4.2 summarizes the predicted moments of inertia.

Table 4.1: Physical parameters used in MATLAB analysis

Parameter	Value	Description
W [m]	0.1	Width of hub
D [m]	0.1	Depth of hub
H [m]	0.02	Height of hub
Q [kg]	0.09	Mass of motor
P [kg]	0.1	Mass of hub
R [m]	0.012	Radius of motor
H [m]	0.036	Height of motor
R [m]	0.25	Distance from motor to hub

Table 4.2: Predicted moment of inertia

	Equation	Value [kg*m <sup>2</sup> ]
J <sub>1</sub>	$(1/3)*Q*(3*r^2+h^2)+4*Q*R^2+(1/12)*P*(H^2+D^2)$	0.026
J <sub>2</sub>	$(1/3)*Q*(3*r^2+h^2)+4*Q*R^2+(1/12)*P*(H^2+D^2)$	0.026
J <sub>3</sub>	$2*Q*r^2+4*Q*R^2+(1/12)*P*(W^2+D^2)$	0.027

Table 4.3 summarizes the values of the initial conditions we used to solve the system of equations along with the parameters in Table 4.1 and Table 4.2.

Table 4.3 Initial conditions used to solve equations in MATLAB simulation

	Name in Code	Value	Description	Units
$x(t=0)$	$x_1$	0	Initial position along x-axis	[m]
$y(t=0)$	$x_3$	0	Initial position along y-axis	[m]
$z(t=0)$	$x_5$	0	Initial position along z-axis	[m]
$\theta(t=0)$	$x_7$	0	Initial pitch	[deg]
$\phi(t=0)$	$x_9$	0	Initial roll	[deg]
$\psi(t=0)$	$x_{11}$	0	Initial yaw	[deg]
$\dot{x}(t=0)$	$x_2$	0	Initial velocity along x-axis	[m/s]
$\dot{y}(t=0)$	$x_4$	0	Initial velocity along y-axis	[m/s]
$\dot{z}(t=0)$	$x_6$	0	Initial velocity along z-axis	[m/s]
$\dot{\theta}(t=0)$	$x_8$	0	Initial rate of change in pitch	[deg/s]
$\dot{\phi}(t=0)$	$x_{10}$	0	Initial rate of change in roll	[deg/s]
$\dot{\psi}(t=0)$	$x_{12}$	0	Initial rate of change in yaw	[deg/s]

### Simulation 1:

When all motors are left at the same thrust (1.3N), the craft rises because the total thrust is larger than the weight of the craft. This is pictured in Figure 4.12. The average climbing speed is 3 m/s. There is no velocity in the xy-plane because the pitch, roll, and yaw are zero.

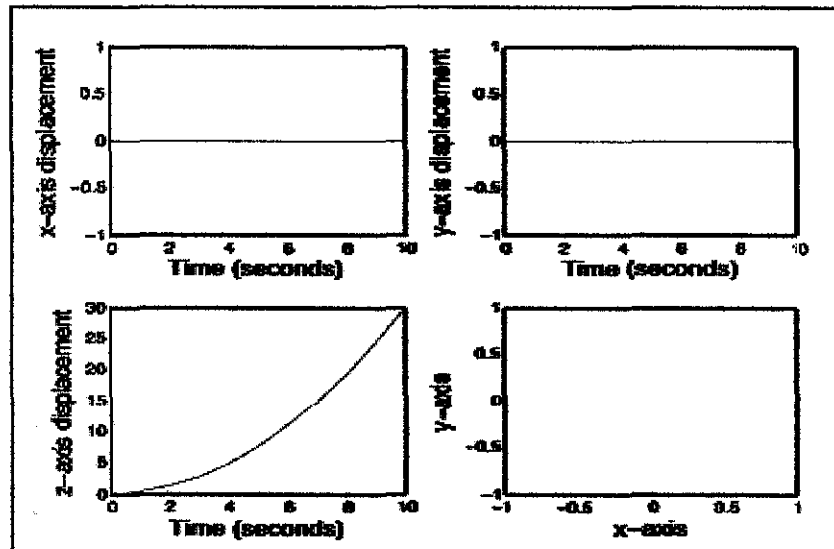


Figure 4.12: First MATLAB simulation results

### Simulation 2:

This simulation represents the movement of the craft when the thrust from motor A is increased by 10% and the thrust from motor C is decreased by 10%. The thrust from motors B and D remains constant. Figure 4.13 displays the expected behavior of the craft.

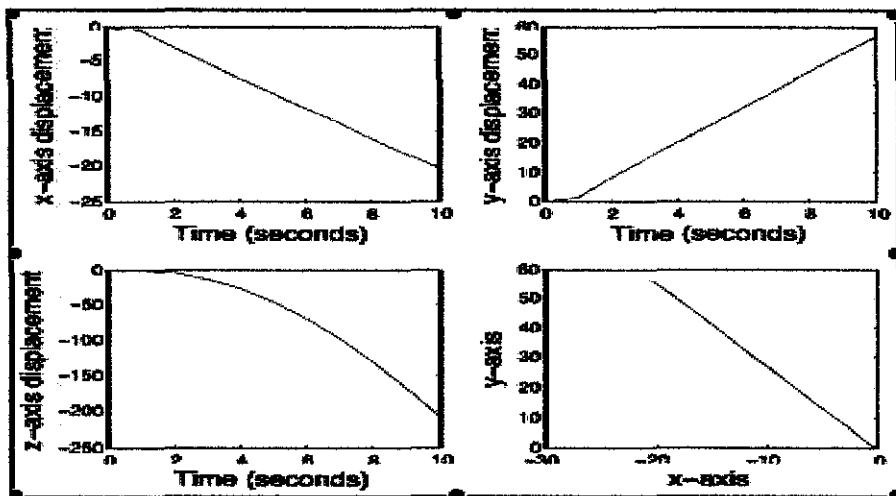


Figure 4.13: Second MATLAB simulation results

The average velocity in the xy-plane is about 5 m/s. The average vertical velocity is 20 m/s in the negative z-direction (falling). It is noteworthy to point out that the craft moved in the xy-plane in the direction predicted from theoretical analysis; however, the craft was also vertically displaced. The drop in height was surprising because I expected the craft to maintain most of its vertical thrust.

### Simulation 3:

I determined that significant velocity can be obtained without a corresponding loss in altitude. Figure 4.14 displays the results of simulated flight when the thrust in motor A is increased by 0.01% and the thrust in motor C is decreased by 0.01%. The average velocity in the xy-plane is about 2 m/s. In this case, the craft continues rising at the same speed as in Simulation 1 (about 3 m/s).

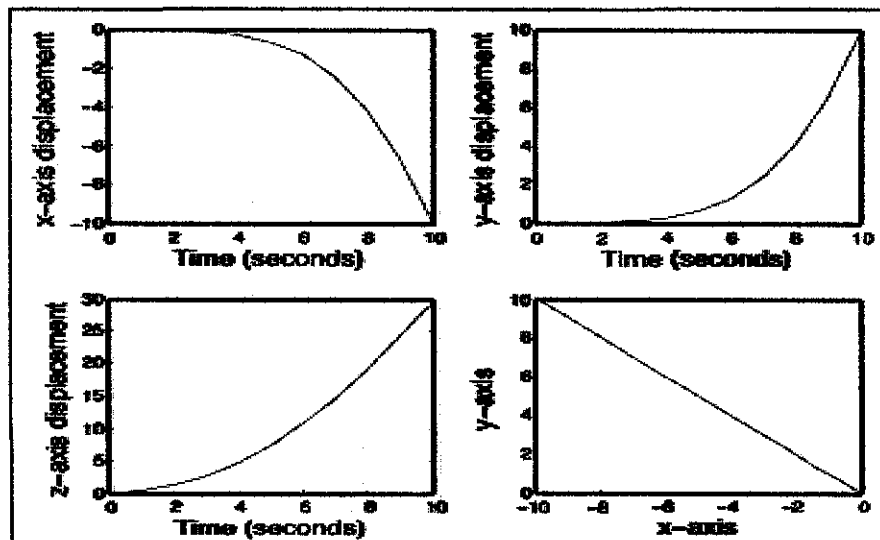


Figure 4.14: Third MATLAB simulation results

Figure 4.13 and Figure 4.14 imply that the craft must be maneuvered with relatively small changes in thrust from each motor. The change in thrust in Simulation 2 is 1000 times larger than the change in thrust in Simulation 3, yet the average velocity in the xy-plane is only 2 or 3 times larger. In addition, the craft continues to rise in simulation 3 but falls fast in simulation 2.

## CHAPTER 5

### CONCLUSION AND RECOMMENDATIONS

#### 5.1 Conclusion

The study on the control system for the MUAV's VTOL operation is very important in providing the best and most suitable control system that can provide the stability to the MUAV's body during the VTOL operation

From this study, the author has selected the control system which consists of a set of sensors, a microchip microcontroller as well as a motor driver. The sensors which include a pair of XY-accelerometer which means to control the MUAV in pitch (X-axis) and roll (Y-axis) angle, a gyroscope that measure the yaw (Z-axis) rate of the MUAV as well as a Ultrasonic (UT) sensor that will provide the MUAV with the altitude control. Besides the sensors, the control system also will use the self-programmable Microchip pic18f4431 processor. The control system coding that have been coded and simulated using the MATLAB software will be embedded into this microchip. The selected microchip also has the onboard high-speed analog digital (A/D) converter and the power pulse width modulation (PWM) module. The module on the microchip will convert the analog signal from the sensors to the digital signal so that it can be read by the motor driver. The motor driver will equally distribute and balance the power to all four of the MUAV's motors so that it can remain stable during take-off and landing operation.

As a conclusion, all the objectives of the study have been achieved. The scope of study stated in the beginning of the project also has been covered by the author.

## **5.2 Recommendations**

### **5.2.1 Physical Control System**

This project basically is only a research-based project where all the outcome results are expected to be only the control system block diagram and the analysis in the form of graph from MATLAB and other any related software. This MUAV project can be improved and enhanced when the real physical control system can be established. Some of the devices such as sensors, accelerometer, camera and gyroscope can be combined to build one operational control system so that further analysis can be performed and the better and more accurate result can be obtained.

The establishment of the physical control system will enable the real-time experiment for the stability analysis of the MUAV body during VTOL operation. The real-time stability analysis will give more accurate readings in term of the euler angles, angular rates, position of the MUAV as well as the velocities reading for each and every motor of the MUAV.

### **5.2.2 Physical Model**

The establishment of the physical control system of the MUAV will not give any meaning if there is no physical body to embed it with. The building processes of the physical model of the MUAV body will cover the building of the structural body of the MUAV which includes the outer body of the MUAV and the chassis of the MUAV. Besides, the physical model of the MUAV also needs the lifting mechanism to fly the body which include the motor and rotors installation.

The biggest obstacle in realizing the physical model of the MUAV will surely be the financial factor. But, in effort in making the first ever MUAV's prototype model comes into reality, the contribution from all parties including the university and the department are really essential.



## REFERENCES

### Journal & Research Studies

- [1] Castillo C. L., Alvis W., Castillo-Effen M., Moreno W., and Valavanis K., 2005, *Small Scale Helicopter Analysis and Controller Design for Non-Aggressive Flight*, Proceedings, IEEE International Conference on Systems, Man and Cybernetics, Florida, USA
  
- [2] Hyondong Oh, Dae-Yeon Won, Sung-Sik Huh, David Hyunchul Shim and Min-Jea Tahk, 2010, *Experimental Framework for Controller Design of a Rotorcraft Unmanned Aerial Vehicle Using Multi-Camera System*, Int'l J. of Aeronautical & Space Science, Daejeon, Korea
  
- [3] Tomasso Bresciani, 2008, *Modelling, Identification and Control of a Quad rotor Helicopter*, Master Thesis, Lund University, Sweden
  
- [4] Samir Boabdallah, Pierpaolo Murrieri, Roland Siegwart, 2003, *Design and Control of an Indoor Micro Quadroto*, Swiss Federal Institute of Technology Lausanne, Switzerland.
  
- [5] Norhidayah Binti Mohd Saini, 2009, *Design of Micro Aerial Vehicle Vertical Take-Off and Landing Mechanism*, Final Year Project Dissertation, Universiti Teknologi PETRONAS, Malaysia
  
- [6] Abdelhamid Tayebi and Stephen McGilvray, 2006, *Attitude Stabilization of a VTOL Quadroto Aircraft*, IEEE Transactions on Control Systems Technology, Canada
  
- [7] Arda Ozgur Kivrak, 2006, *Design of Control Systems for a Quadroto Flight Vehicle Equipped With Inertial Sensors*, Master Thesis in Mechatronics Engineering, Atilim University, Turkey

[8] Carlo Canetta, Jonathan Chin, Sevan Mehrabian, Ludguier Montejo, Hendrik Thompson, 2007, *Quad-rotor Unmanned Aerial Vehicle*, MECE E3410.001: Engineering Design Final Report, Columbia University, USA.

[9] M. Araki, 2010, *Control Systems, robotics and automation*, Encyclopedia of Life Support Systems (EOLSS), USA

[10] E. Altug, J. P. Ostrowski and R. Mahony, 2002, *Control of a Quadrotor Helicopter using Visual Feedback*, Proceedings of the 2002 IEEE International Conference on Robotics and Automation, Washington, DC, USA

### **Books**

[11] Kimon P. Valavanis, 2007, *Advances in Unmanned Aerial Vehicles: State of the Art and the Road to Autonomy*, Springer, The Netherlands.

[12] Bahram Shahian and Michael Hassul, 1993, *Control System Design Using MATLAB*, Prentice Hall, New Jersey, USA.

[13] Dean Frederick and Joe Chow, 2000, *Feedback Control Problems Using MATLAB and the Control System Toolbox*, Brooks/Cole Thomson Learning, California, USA.

[14] Roy Langton, 2006, *Stability and Control of Aircraft System: Introduction to Classical Feedback System*, John Wiley & Sons Ltd., Sussex, England.

[15] Robert F. Stengel, 2004, *Flight Dynamics*, Princeton University Press, USA.

[16] Jan Roskam, 2001, *Airplane Design: Determination of Stability, Control and Performance Characteristics: FAS and Military Requirements*, DAR Corporation, USA.

[17] William Bolton, 2003, *Mechatronics: electronic control systems in mechanical and electrical engineering*, Pearson Prentice Hall, USA.

[18] Michael Barr, 2001, *Pulse Width Modulation, Embedded Systems Programming*, O'Reilly Media, Inc., USA.

[19] Kimon P. Valvanis, 2006, *Advances in Unmanned Aerial Vehicles – State of the Art and the Road to Autonomy*, Springer, The Netherlands.

[20] Tesla, David Hatcher Childress, 1993, *The Fantastic Inventions of Nikola Tesla*, Adventures Unlimited Press, USA

#### **Online Database**

[21] NASA, National Aeronautics and Space Administration Website (2010), Roll Aircraft, Retrieved October 25, from <http://www.grc.nasa.gov/WWW/K-12/airplane/roll.html>

[22] NASA, National Aeronautics and Space Administration Website (2010), Pitch Motion, Aircraft, Retrieved October 25, from <http://www.grc.nasa.gov/WWW/K-12/airplane/pitch.html>

[23] NASA, National Aeronautics and Space Administration Website (2010), Pitch Motion, Aircraft, Retrieved October 25, from <http://www.grc.nasa.gov/WWW/K-12/airplane/yaw.html>

[24] The Curtiss-Wright X-19 VTOL Aircraft (2010)  
[www.456fis.org/CURTISS\\_WRIGHT\\_X-19.html](http://www.456fis.org/CURTISS_WRIGHT_X-19.html)

[25] Draganflyer X4 Four Rotor UAV Helicopter (2010), retrieved October 27, from <http://www.rctoys.com/rc-toys-and-parts/DF-X4-BASE-PKG/RC-HELICOPTERS.html>

[26] PIC18F4431 microchip information (2011), retrieved July 1, from <http://www.microchip.com/wwwproducts/Devices.aspx?dDocName=en010291>

- [27] Introduction to Pulse Width Modulation (PWM) (2011), retrieved July 5, from <http://www.netrino.com/Embedded-Systems/How-To/PWM-Pulse-Width-Modulation>
- [28] Simple PWM Controller, retrieved July 6, from <http://www.nomad.ee/micros/pwm555.html>
- [29] ode45 - Differential Equation Solver, retrieved June 15, from <http://www.math.purdue.edu/~shen/cs614/projects/ode45.pdf>
- [30] Introduction to C/C++, retrieved June 17, from <http://www.learncpp.com/cpp-tutorial/03-introduction-to-cc/>
- [31] The UAV, Unmanned Aerial Vehicle website (2010), retrieved August 8, from <http://www.theuav.com/>
- [32] Monash, The 'Aerial Target' and 'Aerial Torpedo' in the USA, retrieved August 9 from [http://www.ctie.monash.edu.au/hargrave/rpav\\_usa.html](http://www.ctie.monash.edu.au/hargrave/rpav_usa.html)
- [33] Control Tutorial for MATLAB, PID Tutorial (1997), retrieved June 15 from <http://www.engin.umich.edu/group/ctm/PID/PID.html>
- [34] Hubfaces, Sukhoi Su-30 MKI - Purpose of Thrust Vectoring (2006), retrieved June 14, from <http://soni2006.hubpages.com/hub/Thrust-Vectoring-Sukhoi>

## APPENDICES

### A1 – Project Milestone for Final Year I

No.	Detailed Work	1	2	3	4	5	6	7	8	9	10	11	12	13	14
1	<b>Selection of Project Topic</b>														
2	<b>Preliminary Research Work :</b> <ul style="list-style-type: none"> <li>• Collect literatures review</li> <li>• Preliminary interpretation</li> </ul>														
3	<b>Submission of Preliminary Report</b>						●								
4	<b>Project Work :</b> <ul style="list-style-type: none"> <li>• Study on possible control systems</li> <li>• Preliminary control system concept</li> </ul>														
5	<b>Submission of Progress Report</b>								●						
6	<b>Seminar (Compulsory)</b>								●						
7	<b>Project Work Continues :</b> <ul style="list-style-type: none"> <li>• Study on the modeling simulation concept of the MUAV</li> <li>• Study on the control allocation of the MUAV</li> </ul>														
8	<b>Submission of Interim Report</b>														●
9	<b>Oral Presentation</b>														●
<b>During Study Week</b>															

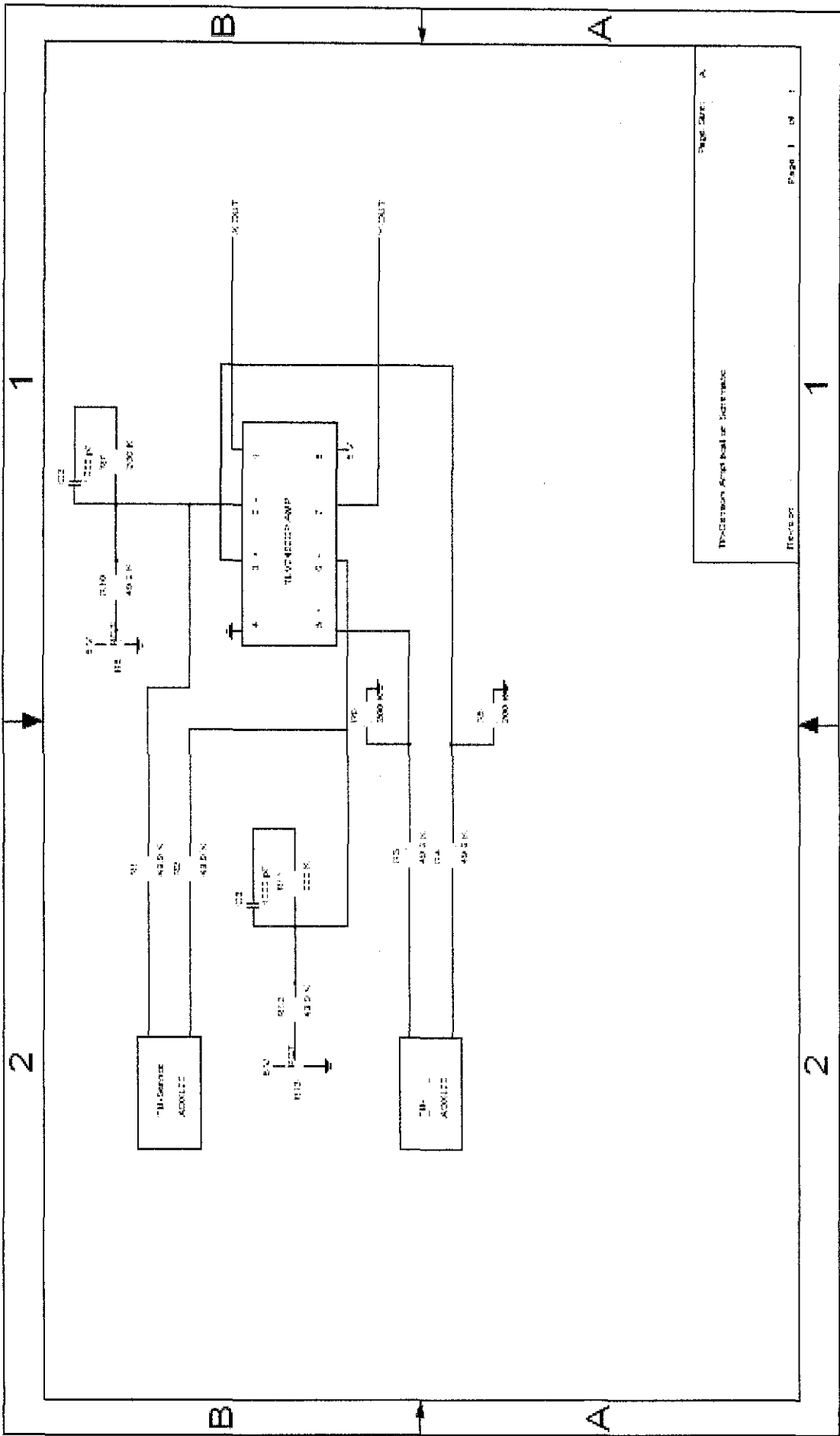
## A2 – Project Milestone for Final Year II

No.	Detailed Work	1	2	3	4	5	6	7	8	9	10	11	12	13	14	15	
1	Literature review																
2	Project Work (Quad Rotor Design and Dynamic Study) • Structure review Control review																
3	Project Work (Control Allocation) • Control System Model Study • Programming (Mathematic equation derivation, I/O parameters identification, control system coding) • Simulation (simulate the control system and extract any related figures or graphs) • Result revision																
4	Submission of Progress Report								●								
5	Project Work Compilation • Revision and compilation of project work • Preparation of Project Poster • Preparation of Dissertation • Preparation of Technical Report																
6	Pre – EDX											●					
7	Submission of Draft Report												●				
8	Submission of Project Dissertation (Soft Bound)													●			
9	Submission of Technical Report												●				
10	Oral Presentation														●		
11	Submission of Project Dissertation (Hard Bound)															●	

### **A3 - Circuit Diagram**

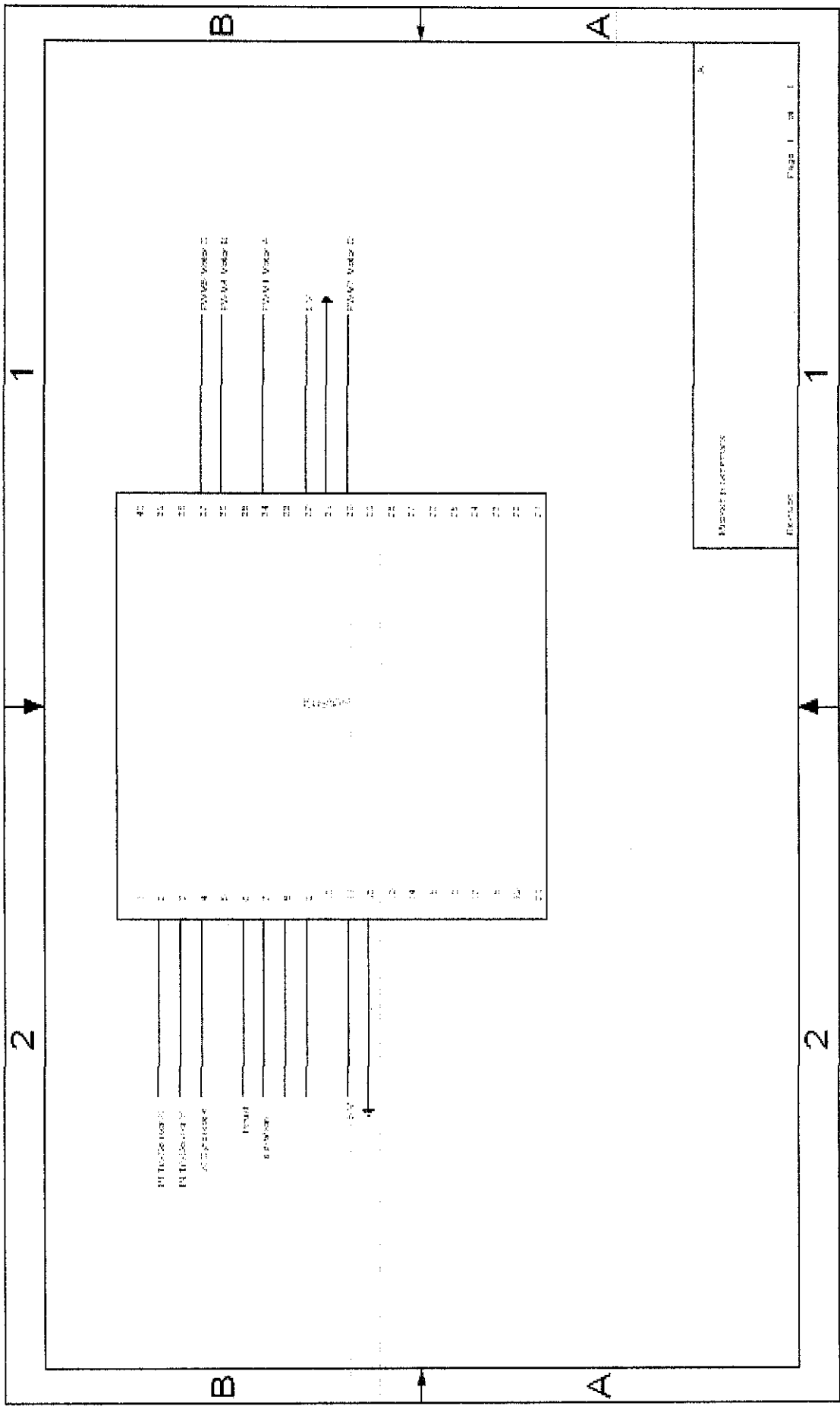


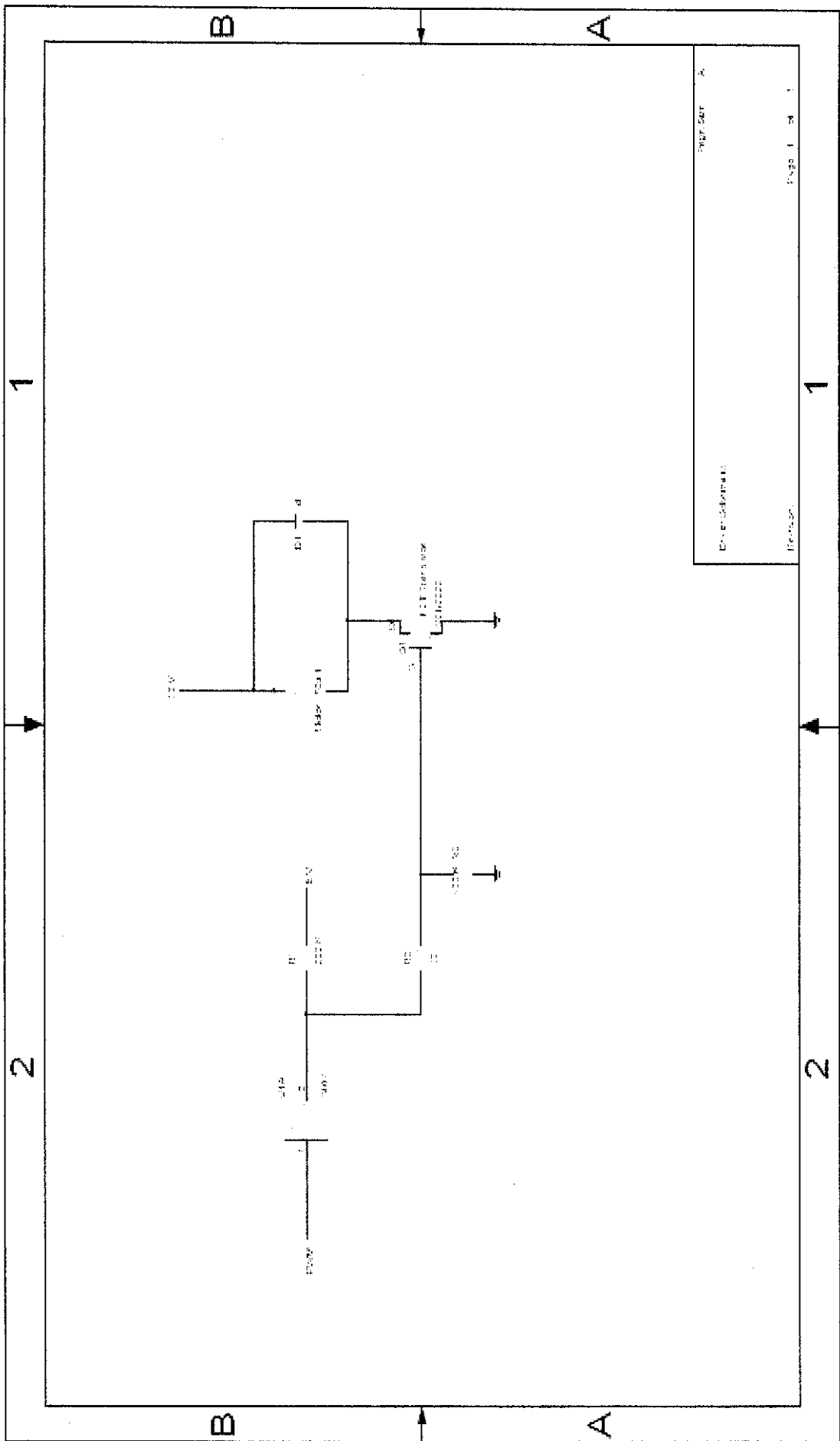


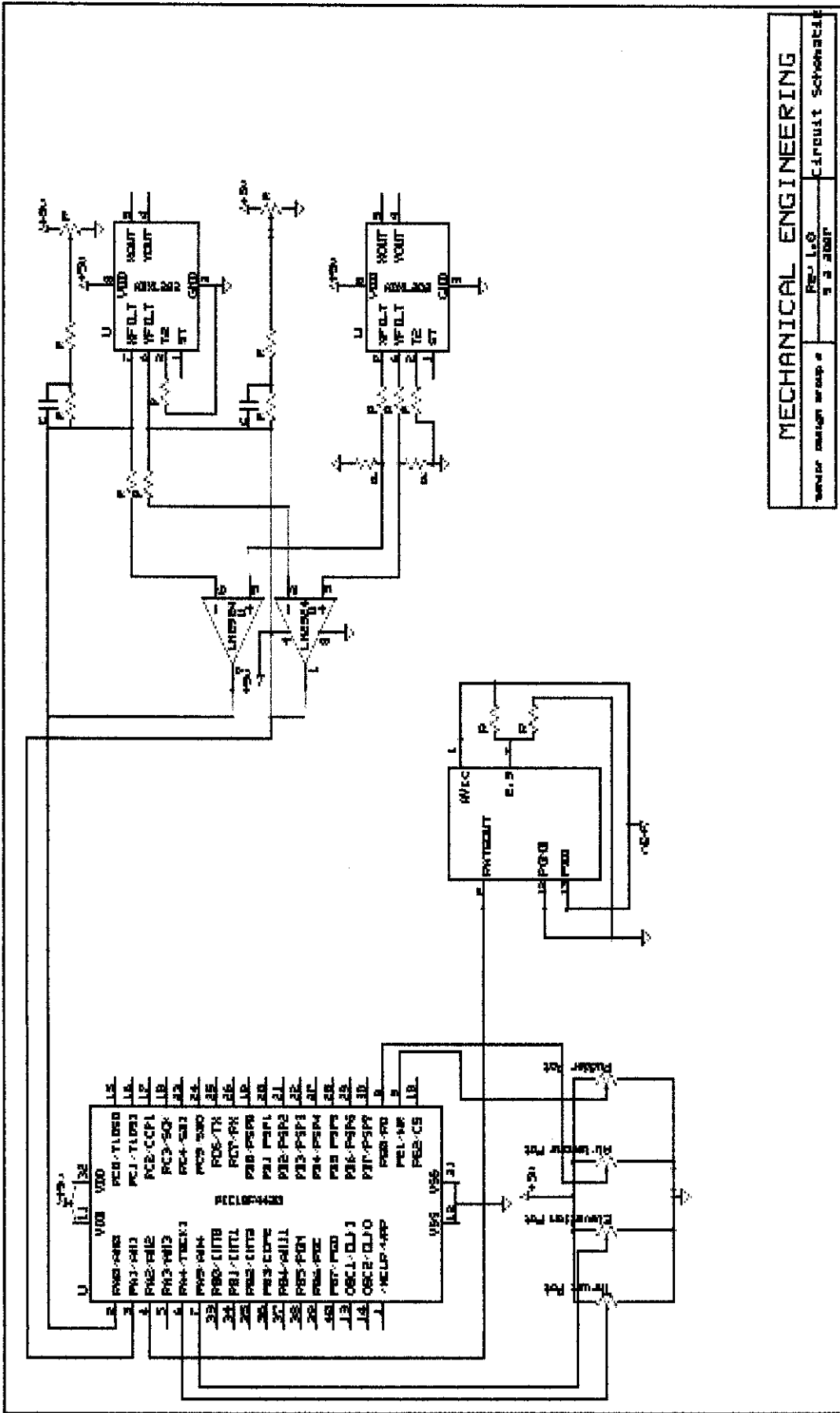


The Circuitry Angel Board for SDR-1000

Page 1 of 1







MECHANICAL ENGINEERING  
 Project No. 100  
 Circuit Schematic

## A4 – Simulation Code

### MATLAB Simulation Code

```
%Driver file
clear all;
close all;
global C g L m J1 J2 J3 F1 F2 F3 F4 nF1 nF2 nF3 nF4 %define global variables
W=0.1;%width of hub
D=W;%depth of hub
H=0.02;%height of hub
Q=0.09;%mass of motor
P=0.1;%mass of hub
r=0.012;%radius of motor
h=0.036;%height of motor
R=0.25;%distance from motor to hub
%constants used in the equations of motion
C=1;
g=9.8;
L=0.2;
m=0.5;
J1=(1/3)*Q*(3*r^2+h^2)+4*Q*R^2+(1/12)*P*(H^2+D^2)
J2=J1
J3=2*Q*r^2+4*Q*R^2+(1/12)*P*(W^2+D^2)
tf = 10; %length of time the ODE's will be solved for
%following is the IC's code, but it wont be use here because there is code
%for it later down, but its kept for referenrece in future use
% x10=100; x20=0; x30=100; x40=0; x50=0; x60=0;
% x70=0; x80=0; x90=0; x100=0; x110=0; x120=0;
% f1a=1.4;f2a=1.4;f3a=1.42;f4a=1.42;
%command code for the craft to go on a trapezoidal path
for j=1:5
if j==1 f1a=1.1;f2a=1;f3a=0.9;f4a=1; end
if j==2 f1a=1.1;f2a=1.1;f3a=0.9;f4a=0.9; end
if j==3 f1a=1;f2a=1.1;f3a=1;f4a=0.9; end
if j==4 f1a=0.9;f2a=0.9;f3a=1.1;f4a=1.1; end
if j==5 f1a=0.9;f2a=0.9;f3a=1.1;f4a=1.1; end

%magnitude of the thrust forcest
F1=1.3*f1a;
F2=1.3*f2a;
F3=1.3*f3a;
F4=1.3*f4a;
%Initial Conditions actually used
if j==1
x10=0; x20=0; x30=0; x40=0; x50=0; x60=0;
x70=0; x80=0; x90=0; x100=0; x110=0; x120=0;
end
if j>1
x10=x1(tf+1,1); x20=0; x30=x1(tf+1,3); x40=0; x50=0; x60=0;
```

```

x70=0; x80=0; x90=0; x100=0; x110=0; x120=0;
end
%File of ODE's
function dx=equations(t,x)
global C g L m J1 J2 J3 F1 F2 F3 F4 nF1 nF2 nF3 nF4
dx=zeros(12,1);
N=1;
dx(1) = x(2);%x dot
dx(2) = ((F1+F2+F3+F4)/m)*(cos(x(11))*sin(x(7))*cos(x(9))+sin(x(11))*sin(x(9)));%x double
dot
dx(3) = x(4);%y dot
dx(4) = ((F1+F2+F3+F4)/m)*(sin(x(11))*sin(x(7))*cos(x(9))-cos(x(11))*sin(x(9)));%y double
dot
dx(5) = x(6);%z dot
dx(6) = ((F1+F2+F3+F4)/m)*(cos(x(7))*cos(x(9)))-g;%z double dot
dx(7) = x(8);%theta dot
dx(8) = ((-F1-F2+F3+F4)/J1)*L;%theta double dot
dx(9) = x(10);%psi dot
dx(10) = ((-F1+F2+F3-F4)/J2)*L;%psi double dot
dx(11) = x(12);%phi dot
dx(12) = C*(F1-F2+F3-F4)/J3;%phi double dot

```

## C-Code for Proportional Control System

```
#include <p18f4431.h>
/*****
pic184431_commented_final.c
This program allows for the control of a quadrotor helicopter.
In particular, the program controls four DC motors via four
individual PWM modules.
The PWM output values for the four motors are determined based
on A/D readings from four inputs and four sensors. The inputs
characterize the desired motion of the craft (thrust, elevator,
aileron, rudder controls). The sensors characterize the actual
motion of the craft (pitch, roll, yaw, altitude). The code
contains equations which account for these 8 inputs to calculate
for the appropriate outputs to each motor.
The program makes use of 8 of the 9 available A/D inputs on the
pic18f4431, as well as the odd PWM output pins (1,3,5,7) for
four unique PWM outputs.
*****/
// variable declarations
signed char kThrust, kElevator, kAilerons, kRudder;
signed char kTiltX, kTiltY, kGyroZ, kSonicZ;
signed int inTiltX=0, inTiltY=0, inGyroZ=0, inSonicZ=0;
signed int inThrust=0, inElevator=0, inAilerons=0, inRudder=0;
signed int outMotorA=0, outMotorB=0, outMotorC=0, outMotorD=0;
signed int testAH=0, testAL=0, testBH=0, testBL=0, testCH=0, testCL=0, testDH=0,
testDL=0;
unsigned int samplecount, limit;
signed int inTiltXsum=0, inTiltYsum=0, inGyroZsum=0, inSonicZsum=0, i, samples;
void DelayFn(unsigned int cnt) // time delay function
{
while (cnt>=1)
{
cnt--;
}
}
void AtoDinit(void)
{
RCONbits.IPEN = 0; // disables priority levels on interrupts
INTCONbits.GIE = 1; // enables global interrupts
INTCONbits.PEIE = 1; // enables peripheral interrupts
PIE1bits.ADIE = 1; // enables A/D interrupt
PIR1bits.ADIF = 0; // ensures that A/D interrupt flag is cleared
ADCON0 = 0b00010100; // enables A/D Module and sets A/D to single shot,
multichannel,
sequential mode, with GO/DONE bit ADCON0<1> cleared, (waiting to be set to start
A/D conversions)
```

```

ADCON1 = 0b00011000; // sets internal Vref+ and Vref-, buffer on
ADCON2 = 0b10110000; // sets A/D acquisition time to 12Tad, clock sets acq time to
Fosc/2, sets right-justified A/D result
ADCON3 = 0b10000000; // interrupt generated on 4th word written to buffer, triggers
disabled
ANSEL0 = 0b11110111; // sets only analog inputs AN0-AN2,AN4-AN7 as enabled,
other pins remain digital I/O status (if ultrasonic used, AN3 needs to be enabled)
ANSEL1 = 0b00000000; // see above-- disables analog input AN8 to maintain digital
I/O status
ADCON0bits.ADON = 1; // turns on A/D module
DelayFn(500); // module requires delay before sampling can be done
}
void AtoDreadSensors(void) // channel select => read sensors (AN0,AN1,AN2,AN3)
{
ADCHS = 0b00000000; // sets analog input pins to their respective sampling groups to
read sensors
DelayFn(10); // time delay necessary when switching channels of the A/D
ADCON0bits.GO_DONE = 1; // starts A/D sampling
while (ADCON0bits.GO_DONE==1) {} // A/D still converting
testAH = ADRESH;
testAL = ADRESL;
inTiltXsum = inTiltXsum + 256*testAH + testAL; // stores reading from tilt sensor X
output
testBH = ADRESH;
testBL = ADRESL;
inTiltYsum = inTiltYsum + 256*testBH + testBL; // stores reading from tilt sensor Y
output
testCH = ADRESH;
testCL = ADRESL;
inGyroZsum = inGyroZsum + 256*testCH + testCL; // stores reading from yaw rate
gyro
testDH = ADRESH;
testDL = ADRESL;
inSonicZsum = inSonicZsum + 256*testDH + testDL; // stores reading from sonic
sensor
}
void AtoDreadInputs(void) // channel select => read inputs (AN4,AN5,AN6,AN7)
{
ADCHS = 0b01010101; // sets analog input pins to their respective sampling groups to
read inputs
DelayFn(10); // time delay necessary when switching channels of the A/D
ADCON0bits.GO_DONE = 1; // starts A/D sampling
while (ADCON0bits.GO_DONE==1) {} // A/D still converting
testAH = ADRESH;
testAL = ADRESL;
inThrust = 256*testAH + testAL; // stores reading from thrust input

```



```

testBH = ADRESH;
testBL = ADRESL;
inElevator = 256*testBH + testBL; // stores reading from elevator input
testCH = ADRESH;
testCL = ADRESL;
inAilerons = 256*testCH + testCL; // stores reading from aileron input
testDH = ADRESH;
testDL = ADRESL;
inRudder = 256*testDH + testDL; // stores reading from rudder input
}
void PWMinit(void)
{
PTCON0 = 0b00000000; // 1:1 Prescale & 1:1 Postscale
PTCON1 = 0b00000000; // Time Base Timer options PTCON1<7>=PTEN = time base
enable bit [makes it go]
PWMCON0 = 0b01111111; // enables all PWM pins (RB1,RB3,RB5,RD7) and
sets independent mode
PWMCON1 = 0b00000000; // other pwm inits
PTPERH = 0x00; // sets PTPER to FFh (10-bit PWM resolution, 39.6 kHz
frequency)
PTPERL = 0xFF;
}
void PWMout(void)
{
//for the tilt+gyro inputs, the equilibrium value is 2.5V/5V-- as such, a no-change
tilt/gyro reading should
be read as .5(10-bit resolution) = 512.
//for the inElevator, inAilerons, inRudder inputs, equilibrium value is 2.5V/5V, for the
inThrust, the
equilibrium value is 0V/5V.
outMotorA = (kThrust*(inThrust) - (kElevator*(inElevator-512) + kTiltX*(inTiltX-
512)) -
(kRudder*(inRudder-512) + kGyroZ*(inGyroZ-512)));
if (inThrust < limit)
{
outMotorA=0;
PDC0L = 0b00000000;
PDC0H = 0b00000000;
}
else if (inThrust > limit && outMotorA < limit)
{
if (limit > 255)
{
PDC0L = limit;
PDC0H = 0b00000001;
}
}
}

```

```

else if (limit < 255)
{
PDC0L = limit;
PDC0H = 0b00000000;
}
}
else if (inThrust > limit && outMotorA > 1023)
{
PDC0L = 0b11111111;
PDC0H = 0b00000011;
}
else if (inThrust > limit && outMotorA > limit && outMotorA < 256)
{
PDC0L = outMotorA;
PDC0H = 0b00000000;
}
else if (inThrust > limit && outMotorA > 255 && outMotorA < 512)
{
PDC0L = outMotorA - 256;
PDC0H = 0b00000001;
}
else if (inThrust > limit && outMotorA > 511 && outMotorA < 768)
{
PDC0L = outMotorA - 512;
PDC0H = 0b00000010;
}
else if (inThrust > limit && outMotorA > 767 && outMotorA < 1024)
{
PDC0L = outMotorA - 768;
PDC0H = 0b00000011;
}
outMotorB = (kThrust*(inThrust) + (kAilerons*(inAilerons-512) + kTiltY*(inTiltY-
512)) +
(kRudder*(inRudder-512) + kGyroZ*(inGyroZ-512)));
if (inThrust < limit)
{
outMotorB=0;
PDC1L = 0b00000000;
PDC1H = 0b00000000;
}
else if (inThrust > limit && outMotorB < limit)
{
if (limit > 255)
{
PDC1L = limit;
PDC1H = 0b00000001;
}
}

```

```

}
else if (limit < 255)
{
PDC1L = limit;
PDC1H = 0b00000000;
}
}
else if (inThrust > limit && outMotorB > 1023)
{
PDC1L = 0b11111111;
PDC1H = 0b00000011;
}
else if (inThrust > limit && outMotorB > limit && outMotorB < 256)
{
PDC1L = outMotorB;
PDC1H = 0b00000000;
}
else if (inThrust > limit && outMotorB > 255 && outMotorB < 512)
{
PDC1L = outMotorB - 256;
PDC1H = 0b00000001;
}
else if (inThrust > limit && outMotorB > 511 && outMotorB < 768)
{
PDC1L = outMotorB - 512;
PDC1H = 0b00000010;
}
else if (inThrust > limit && outMotorB > 767 && outMotorB < 1024)
{
PDC1L = outMotorB - 768;
PDC1H = 0b00000011;
}
outMotorC = (kThrust*(inThrust) - (kAilerons*(inAilerons-512) + kTiltY*(inTiltY-
512)) +
(kRudder*(inRudder-512) + kGyroZ*(inGyroZ-512)));
if (inThrust < limit)
{
outMotorC=0;
PDC2L = 0b00000000;
PDC2H = 0b00000000;
}
else if (inThrust > limit && outMotorC < limit)
{
if (limit > 255)
{
PDC2L = limit;

```

```

PDC2H = 0b00000001;
}
else if (limit < 255)
{
PDC2L = limit;
PDC2H = 0b00000000;
}
}
else if (inThrust > limit && outMotorC > 1023)
{
PDC2L = 0b11111111;
PDC2H = 0b00000011;
}
else if (inThrust > limit && outMotorC > limit && outMotorC < 256)
{
PDC2L = outMotorC;
PDC2H = 0b00000000;
}
else if (inThrust > limit && outMotorC > 255 && outMotorC < 512)
{
PDC2L = outMotorC - 256;
PDC2H = 0b00000001;
}
else if (inThrust > limit && outMotorC > 511 && outMotorC < 768)
{
PDC2L = outMotorC - 512;
PDC2H = 0b00000010;
}
else if (inThrust > limit && outMotorC > 767 && outMotorC < 1024)
{
PDC2L = outMotorC - 768;
PDC2H = 0b00000011;
}
outMotorD = (kThrust*(inThrust) + (kElevator*(inElevator-512) - kTiltX*(inTiltX-
512)) -
(kRudder*(inRudder-512) + kGyroZ*(inGyroZ-512)));
if (inThrust < limit)
{
outMotorD=0;
PDC3L = 0b00000000;
PDC3H = 0b00000000;
}
else if (inThrust > limit && outMotorD < limit)
{
if (limit > 255)
{

```

```

PDC3L = limit;
PDC3H = 0b00000001;
}
else if (limit < 255)
{
PDC3L = limit;
PDC3H = 0b00000000;
}
}
else if (inThrust > limit && outMotorD > 1023)
{
PDC3L = 0b11111111;
PDC3H = 0b00000011;
}
else if (inThrust > limit && outMotorD > limit && outMotorD < 256)
{
PDC3L = outMotorD;
PDC3H = 0b00000000;
}
else if (inThrust > limit && outMotorD > 255 && outMotorD < 512)
{
PDC3L = outMotorD - 256;
PDC3H = 0b00000001;
}
else if (inThrust > limit && outMotorD > 511 && outMotorD < 768)
{
PDC3L = outMotorD - 512;
PDC3H = 0b00000010;
}
else if (inThrust > limit && outMotorD > 767 && outMotorD < 1024)
{
PDC3L = outMotorD - 768;
PDC3H = 0b00000011;
}
}
}
// Notes: PWM duty cycles and inputs are 10-bits. to have it hover, we either need to
calculate how much it weighs
relative to a particular thrust or have some sort of input sensor to tell us vertical
movement. thus, to make it hover
for this initial program, we need to experiment with what exactly is the PWM duty
cycle that makes it just lift off
(which would also be the hovering duty cycle).
void main(void)
{
//%%%%%%%%%%
%%%%%%%%%

```



